

THE PERFORMANCE OF RAYLEIGH FAST-
FADING CHANNELS WITH INTERSYMBOL INTERFERENCE AND
ADDITIVE GAUSSIAN NOISE

A Thesis Presented to the
Faculty of the Department of
Electrical Engineering
University of Houston

In Partial Fulfillment of the
Requirements for the Degree
Master of Science in Electrical Engineering

by
Howard H. Ma
May 1978

THE PERFORMANCE OF RAYLEIGH FAST-
FADING CHANNELS WITH INTERSYMBOL INTERFERENCE AND
ADDITIVE GAUSSIAN NOISE

An Abstract of a Thesis
Presented to
the Faculty of the Department of Electrical Engineering
University of Houston

In Partial Fulfillment
of the Requirements for the Degree
Master of Science in Electrical Engineering

by
Howard H. Ma
May 1978

ABSTRACT

Presented herein is an analysis of the effects of intersymbol interference on the performance of digital communication systems operating over channels corrupted by Rayleigh fast-fading and additive Gaussian noise. The results are applicable to systems employing coherent detection schemes.

For mean signal-to-noise ratios of 15 dB or less, and for typical pulse shapes with reasonably well synchronized sampling, intersymbol interference is shown to contribute no significant amount to the total probability of bit-error over the Rayleigh fast-fading channels. (The fraction of bit error rate due to intersymbol interference is less than 0.2 of the total bit-error probability for most cases) As the mean signal-to-noise ratio is increased to higher levels, the effects of intersymbol interference on the performance of the digital communication systems become more significant. For mean signal-to-noise ratios of 25 dB or more, the incremental bit-error probability caused by intersymbol interference begins to play a dominant part of the total bit-error probability over the bit-error rate due to additive noise alone. For mean signal-to-noise ratios of 45 dB or more, the total bit-error probability is almost entirely due to intersymbol interference. An irreducible error rate is created thereafter due to the severity of intersymbol interference. Such results are different from those obtained in the absence of fading, in which case the bit-error

probability at signal-to-noise ratios in excess of 15 dB is almost entirely due to intersymbol interference. They also contrast sharply with those obtained in Rayleigh slow-fading channels where the incremental bit-error probability caused by intersymbol interference is seen to be limited to some small fractional part of the total bit-error probability as the mean signal-to-noise ratio is increased to higher levels.

TABLE OF CONTENTS

ABSTRACT	iv
LIST OF FIGURES	viii
LIST OF TABLES	ix
I. INTRODUCTION	1
II. CHARACTERIZATION AND MODELING FOR LINEAR TIME- VARIANT CHANNELS	5
Definition and Characterization of Linear Time- Variant Channels	5
Other Forms for the Impulse Response	6
Separable Time-Variant Systems	7
III. MATHEMATICAL MODEL OF THE COMMUNICATION CHANNEL ..	12
Signal Source	12
Channel Impulse Response	15
Intersymbol Interference	16
Fading	16
Additive Gaussian Noise	18
Decision Element	18
The Conditional Bit-Error Probability	20
Signal-to-Noise Ratio	23
IV. NUMERICAL DETERMINATION OF BIT-ERROR PROBABILITY	
FOR THE RAYLEIGH FAST-FADING CHANNEL	24
Characteristic Function of the Additive Noise	24
Characteristic Function of the Intersymbol Interference	24
Characteristic Function of the Total Distortion ..	27

TABLE OF CONTENTS (concluded)

Integral Equation for the Conditional Bit-Error	
Probability	27
The Small Difference Problem	28
Integral Equation for the Total Bit-Error	
Probability	29
Truncation Error	32
Trapezoidal Integration Rule	34
Determination of Terms Used in the Series	
Expansion	35
Magnitude of Integration Error	36
The Bit-Error Probabilities for the Rayleigh Fast-	
Fading Channel	36
Asymptotic Behavior of P_{e_z}	52
Overall Effects of Intersymbol Interference	
on Total Bit-Error Probability	53
V. CONCLUSION	56
REFERENCES	58
APPENDIX A	62
APPENDIX B1	64
APPENDIX B2	69

LIST OF FIGURES

1. Model of the General Time-Variant Digital System	8
2. Two Elementary Time-Variant Models	10
3. Typical Digital Communication System	13
4. Model of the Typical Digital Communication System	14
5. Performance of Rayleigh Fast-Fading Channel: Gaussian Pulse, $\gamma = 0$	42
6. Performance of Rayleigh Fast-Fading Channel: Gaussian Pulse, $\gamma = 0.1T$	43
7. Performance of Rayleigh Fast-Fading Channel: Gaussian Pulse, $\gamma = 0.2T$	44
8. Performance of Rayleigh Fast-Fading Channel: Gaussian Pulse, $\gamma = 0.3T$	45
9. Performance of Rayleigh Fast-Fading Channel: Gaussian Pulse, $\gamma = 0.4T$	46
10. Performance of Rayleigh Fast-Fading Channel: Chebyshev Pulse, $\gamma = 0$	47
11. Performance of Rayleigh Fast-Fading Channel: Chebyshev Pulse, $\gamma = 0.05T$	48
12. Performance of Rayleigh Fast-Fading Channel: Chebyshev Pulse, $\gamma = 0.1T$	49
13. Performance of Rayleigh Fast-Fading Channel: Chebyshev Pulse, $\gamma = 0.15T$	50
14. Performance of Rayleigh Fast-Fading Channel: Chebyshev Pulse, $\gamma = 0.2T$	51

LIST OF TABLES

1. Convergence of Numerical Integration for the Rayleigh Fast-Fading Channel, Gaussian Pulse	37
2. Convergence of Numerical Integration for the Rayleigh Fast-Fading Channel, Chebyshev Pulse	39
3. Asymptotic Behavior of P_{e_z}/P_e	55

CHAPTER I

INTRODUCTION

The performance of a digital communication system is commonly specified in terms of its bit-error probability for a given signal-to-noise ratio. A number of useful techniques have been developed to determine this performance index for transmission over channels subject to intersymbol interference and additive Gaussian noise [1], [2], [3]. The channel models used in these developments are all assumed to be time-invariant; i.e. channel attenuation of the transmitted signal is invariant with time.

Now the mere fact that a radio transmitter emits a high frequency signal of constant amplitude in no way assures that the signal observed at some distant receiving antenna is of the same steady nature. In practice, the envelop of the received signal is invariably seen to fluctuate in an irregular fashion and may well go through several maxima and minima in a matter of seconds. These fluctuations have been recorded and studied by a number of investigators [4], [5], [6], [7]. For observations extending over a period of fifteen minutes or less, the variations in envelope size tend to follow a Rayleigh distribution, as predicted in the theory for multipath channels [8, pp. 527-532].

Some researchers have evaluated the influences of fading on the bit-error probabilities of binary data transmission systems [9], [10], [11], [12]. But they all assumed a specific

transmission mode or detector during the derivations. In addition, none took the effects of intersymbol interference into considerations.

Vanelli and Shehadeh [13] applied one of the channel models for time-variant systems to evaluate the effects of intersymbol interference on Rayleigh fading channels. They assumed that the fading rate is so slow that fluctuations over several bits may be ignored. This slow fading assumption is removed in this thesis which derives a more general integral expression for the bit-error probability of a Rayleigh fast-fading channel with intersymbol interference and additive Gaussian noise. Then, numerical integration is used to evaluate this integral expression. The amount of digital computer time required is modest.

The development is based on a generalized variation of the binary baseband channel model. In this model, the entire channel response is represented by a single linear filter with a Rayleigh distributed multiplicative perturbation introduced to account for the fast-fading. The input to the filter is an infinite sequence of equiprobable binary impulses. Filtered Gaussian noise is added at the filter output and decisions at the receiver are based on sampled values of this sum. This model is described in detail in Chapter III.

The sampled value of the total distortion introduced by this channel given the fading effect on a specific bit is the random variable which is the sum of the additive noise

plus intersymbol interference observed at each sampling instant. The bit-error probability conditional on the value of the multiplier for that bit can readily be expressed in terms of the probability density function of this random variable. The density function is the Fourier transform of the characteristic function. If the noise and intersymbol interference are statistically independent, then the characteristic function of the total distortion is the product of the characteristic functions of these constituents. This conditional bit-error probability is finally averaged over the ensemble of values of the multiplicative Rayleigh random variable. The result is a formidable looking double-integral expression for the bit-error probability.

The approach used herein is to eliminate one integral by interchanging the order of integration and integrating over fading. Then it is shown that the remaining integral is remarkably easy to evaluate using the simple trapezoidal integration rule.

In Chapters III and IV, the techniques for computing total bit-error probability are derived in detail for the Rayleigh fast-fading channel. Numerical results are obtained and it is seen that the performance degradation due to intersymbol interference on the fading channel becomes very significant and plays a dominant role when the signal-to-noise ratio is increased to higher levels. For a fixed ratio of signal to noise there is an irreducible asymptotic probability of error (even at large values of signal-to-noise ratio, the

bit-error probability can not be reduced below the asymptotic value) beyond which the system performance can not be improved no matter how large the signal-to-noise ratio becomes. These results are discussed in Chapter IV.

Details of the digital computer programs developed to obtain the numerical results are provided in the Appendices.

CHAPTER II

CHARACTERIZATION AND MODELING FOR LINEAR TIME-VARIANT CHANNELS [14]

Definition and Characterization of Linear Time-Variant Channels

A time-variant channel is one whose input-output relationship is not invariant under translations in time. If, in addition, the superposition principle holds for the channel, it is defined as a linear time-variant channel. The most commonly used method of characterizing such a linear time-variant channel is the impulse response of the channel.

The impulse response of a linear time-variant channel is defined as $h_1(t, \tau)$, the output measured at time t in response to a unit impulse applied at time τ . For a physical realizable channel, $h_1(t, \tau)$ is zero for $t < \tau$.

Since the input $x(t)$ can be regarded as being composed of weighted impulses,

$$x(t) = \int_{-\infty}^t x(\tau) \delta(t-\tau) d\tau, \quad (1)$$

we can write the output $y(t)$ by virtue of linearity of the channel,

$$y(t) = \int_{-\infty}^t x(\tau) h_1(t, \tau) d\tau \quad (2)$$

which, for a realizable channel, can also be written as

$$y(t) = \int_{-\infty}^{\infty} x(\tau) h_1(t, \tau) d\tau \quad (3)$$

because $h_1(t, \tau) = 0$ for $t < \tau$.

Note that in a time-invariant system, $h_1(t, \tau)$ would be a function of $(t - \tau)$ only, and not of t or τ separately.

Other Forms for the Impulse Response

In the function $h_1(t, \tau)$ the realizability condition is that the response be identically zero for $t < \tau$. This constraint involves both t and τ , and therefore is often inconvenient to use. In the alternate forms of impulse response now to be described, the realizability condition involves only one variable.

We define

$h_2(z, \tau)$ = response measured at time $t = \tau + z$ to
a unit impulse applied at time τ

$h_3(y, t)$ = response measured at time t to a unit
impulse applied at time $t - y$

where

t : variable corresponding to instant of observation
of response,

τ : variable corresponding to instant of application
of impulse excitation,

z : variable corresponding to elapsed time since
application of input,

y : variable corresponding to age of input.

The notation of $h_2(z, \tau)$ can be said to emphasize the "impulse response" character of the quantity described, z measuring "elapsed time" since the application of the impulse. The $h_3(y, t)$ notation emphasizes the "weight function" character, y measuring the "antiquity" or "age" of the input. The realizability conditions are zero response for $z < 0$ and $y < 0$ respectively. Of course, $h_1(t, \tau)$, $h_2(z, \tau)$ and $h_3(y, t)$ must all be related. The rules governing transformation from one form to another are derived from the relations $z = t - \tau = y$ between the time-domain variables z , t , τ , and y .

Separable Time-Variant Systems

A general time-variant system is given in Figure 1. The received waveform can be written as

$$r(t) = \int_{-\infty}^{\infty} h_1(t, \tau) s(\tau) d\tau + n(t). \quad (4)$$

where $h_1(t, \tau)$ is the combination of transmitter, transmission medium, receiver front-end and detector. For a sampling instant of γ , the zeroth sampled value of the filter output plus noise is

$$r_0 = r(\gamma) = \int_{-\infty}^{\infty} h_1(\gamma, \tau) s(\tau) d\tau + n(\gamma). \quad (5)$$

While some knowledge of the multipath autocovariance

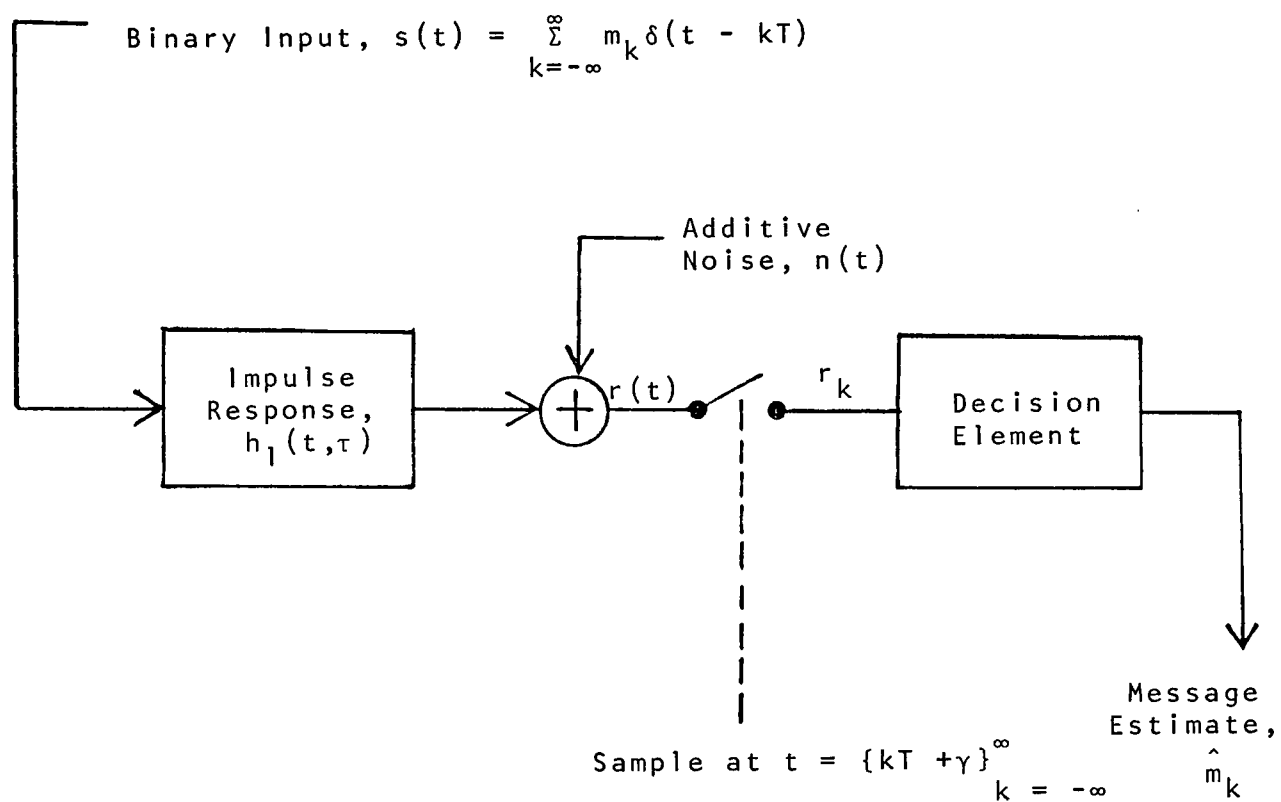


Figure 1. Model of the General Time-Variant Digital System

profile can be obtained from (4) [15], one cannot derive useful general expressions concerning performance without further simplification of the channel model, $h_1(t, \tau)$.

Two elementary forms of linear time-variant filters are of special interest because of their simplicity and usefulness in constructing more complicated linear time-variant filters.

These models are shown in Figure 2. In the first model (Type I) the input $x(t)$ is passed through the linear time-invariant filter $f(t)$ and then multiplied by the function $g(t)$ to give the output $y(t)$. In the second model (Type II) the input is first multiplied by $g(t)$ and then passed through the time-invariant filter $f(t)$.

The impulse response of the Type I model is given by

$$h_1(t, \tau) = f(t - \tau)g(\tau)$$

or

$$h_2(z, \tau) = f(z)g(\tau + z) \quad (6)$$

or

$$h_3(y, t) = f(y)g(t)$$

Notice that these three expressions are of the form

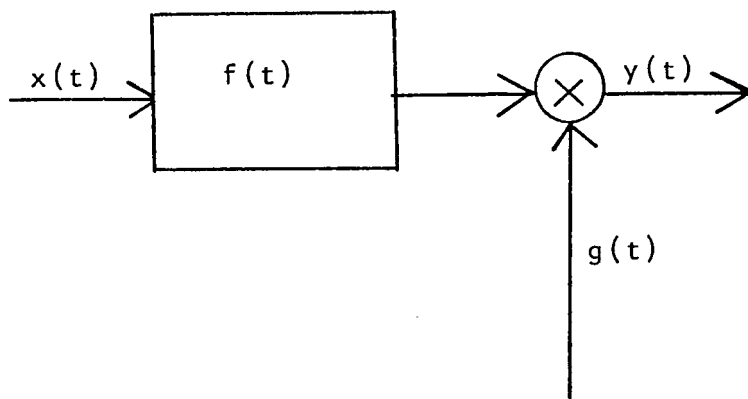
impulse response =

$$f(\text{time elapsed since application of input})g(\text{instant at which output is observed}).$$

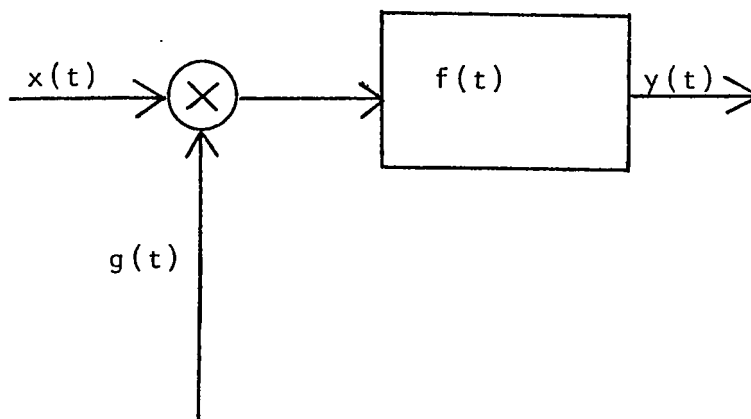
Similarly the impulse response of the Type II model can be expressed in the generic form

impulse response =

$$g(\text{instant at which input is applied})f(\text{time elapsed since application of input}).$$



(a)



(b)

Figure 2. Two Elementary Time-Variant Models

(a) Type I; (b) Type II.

which, in particular, becomes

$$h_1(t, \tau) = g(\tau)f(t-\tau)$$

or

$$h_2(z, \tau) = g(\tau)f(z) \quad (7)$$

or

$$h_3(y, t) = g(t-y)f(y)$$

Because of the form of Eqs. (6) and (7) for $h_3(y, t)$ and $h_2(z, \tau)$, these will be called separable time-variant systems.

Which model we should use for this study depends heavily on the constraints imposed on the channel. If we assume the channel be linear, it can be described conveniently by the impulse response functions. Additional constraints on the channel can now be represented as constraints on these functions.

Two basic assumptions made for the time-variant channel are

1. it is a Rayleigh-fading channel,
2. the multiplication factor $g(t)$ is a piecewise constant function of bit location kT .

The second assumption implies that $g(t)$ is a function of the instant at which input is applied. Thus the channel is modeled as a Type II system. Further details of the model are discussed in Chapter III.

CHAPTER III

MATHEMATICAL MODEL OF THE COMMUNICATION CHANNEL

A simplified block diagram of a typical digital communication system is shown in Figure 3. Such a system may employ amplitude-shift keying (ASK), frequency-shift keying (FSK) or phase-shift keying (PSK). In addition, a number of detectors are available for each of these modes.

The intent of this study is not to evaluate any specific transmission mode or detector, but rather to deal in general with the effects of intersymbol interference on digital communication over fast-fading channels. For this purpose, it is sufficient to model the typical system as shown in Figure 4; i.e. a variation of the familiar binary baseband channel.

Signal Source

The system input is modeled as an infinite sequence of unit amplitude impulses,

$$s(t) = \sum_{k=-\infty}^{\infty} m_k \delta(t - kT) \quad (8)$$

where $\delta(t - w)$ is the unit impulse occurring at time $t = w$. The binary inputs, m_k , are generated with bit rate $1/T$ and are assumed to be equiprobable and statistically independent. That is

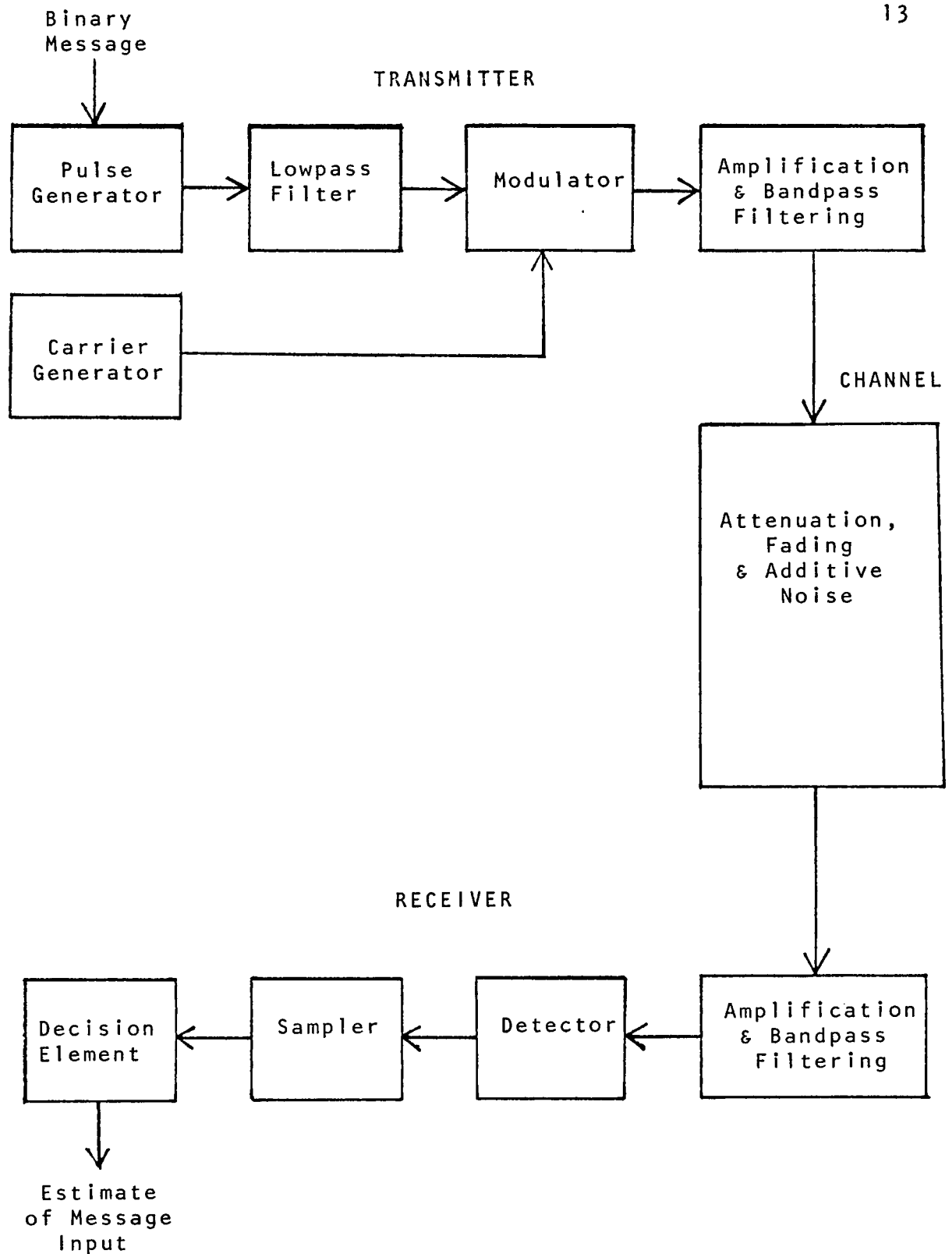


Figure 3. Typical Digital Communication System

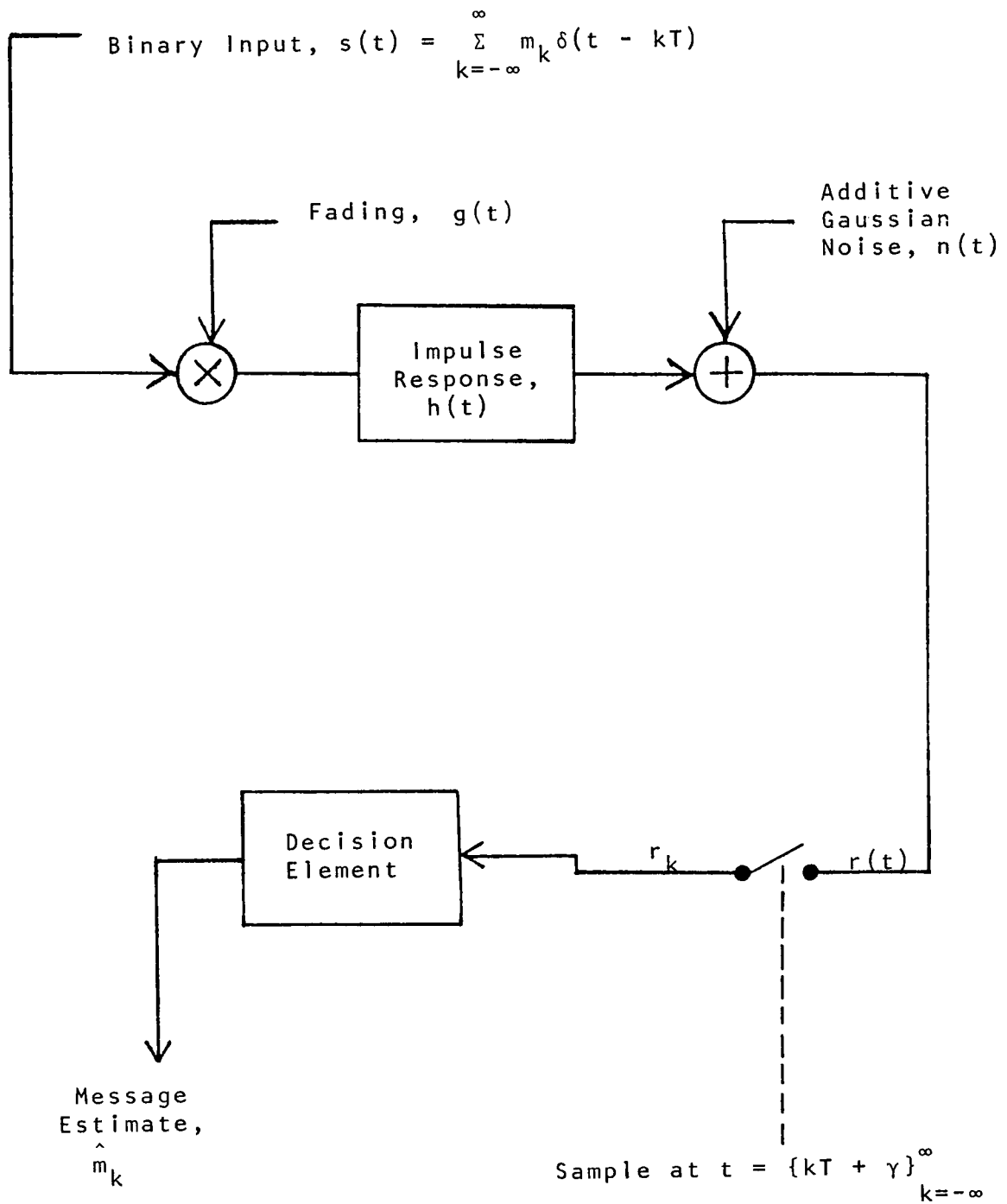


Figure 4. Model of the Typical Digital Communication System

$$\Pr(m_k = 1) = \Pr(m_k = -1) = 0.5,$$

$$\Pr(m_k | m_j) = \Pr(m_k). \quad (9)$$

Channel Impulse Response

The transmitter, transmission medium, receiver front-end and detector are all modeled by a single time-invariant linear filter with square-integrable impulse response, $h(t)$. It is further assumed that $h(t)$ is normalized such that

$$h(0) = 1. \quad (10)$$

It is important to note that inclusion of the detector in the linear filter limits the scope of the model to include only coherent detection schemes. Noncoherent detectors involve non-linear operations which cannot be represented by a linear filter.

Two specific impulse responses are considered in the examples of the next two chapters. The first of these is the Gaussian pulse. This is the limiting shape of a filter composed of passive elements. As the number of elements becomes large, the impulse response very closely approximates the Gaussian shape. It is also the limiting case of maximally flat time-delay approximation as the order increases. For the cases considered herein, the Gaussian pulse is defined by

$$h(t) = \exp[-(8t / 5T)^2]. \quad (11)$$

The other impulse response modeled is that of a fourth-order Chebyshev filter which provides the proper passband ripple and drops very abruptly outside the band. This is an approximation to the impulse response of an ideal bandlimited

filter. For the purposes of this study, the Chebyshev pulse is defined by the expression

$$h(t) = 0.4023 \cos(2.839 t/T - 0.7553) \exp(-0.4587 t/T) + 0.7163 \cos(1.176 t/T - 0.1602) \exp(-1.107 t/T). \quad (12)$$

The reasons to choose these filters are

1. their resemblance to typical impulse responses of linear filters,
2. the results of performance of time-invariant systems and Rayleigh slow-fading channels using these pulses are readily obtained and easily compared with those of this study.

Intersymbol Interference

The signal overlap into adjacent time slots may, if too strong, result in an erroneous decision. This phenomenon of pulse overlap and the resultant difficulty with receiver decisions is termed intersymbol interference.

It is assumed that pulses separated from the main pulse by an interval in excess of KT are greatly attenuated and do not contribute significantly to the intersymbol interference of the main pulse. This is a necessary and reasonable assumption for any practical communication channel [16, pp. 349-366].

Fading

Fading is defined as the noise which can multiply the signal. It is represented by the multiplicative perturbation, $g(t)$. It is assumed that $g(t)$ is positive for all t and constant over each individual bit period; i.e.

$$g_k = g(kT) > 0, \quad k = 0, \pm 1, \pm 2, \dots \pm K. \quad (13)$$

For radio channels subject to purely random multipath interference, the instantaneous amplitude of the received signal can be shown in theory to follow a Rayleigh distribution [6], [7]. Experimental measurements also strongly support this result [4], [5]. Consequently, the Rayleigh fading channel is taken as a reasonable model for the purposes of this study. Then $g(t)$ is described statistically by the density function

$$\begin{aligned}
 P_{g_k}(\beta_k) &= 0, & \beta_k < 0 \\
 & & k = -K, \dots, K \\
 &= \left(\frac{2\beta_k}{\mu_k^2} \right) \exp(-\beta_k^2 / \mu_k^2), \beta_k \geq 0 & (14)
 \end{aligned}$$

where μ_k is the root-mean-squared (RMS) amplitude of $g_k(t)$,

$$\mu_k^2 = E[g_k^2(t)].$$

The operator E denotes the expected value of a random variable.

It is convenient to consider only the particular case:

assume

$$\mu_k = 1 \quad k = -K, \dots, K. \quad (15)$$

On this assumption, (14) becomes

$$\begin{aligned}
 P_{g_k}(\beta_k) &= 0, & \beta_k < 0 \\
 & & k = -K, \dots, K. \\
 &= 2\beta_k \exp(-\beta_k^2), \beta_k \geq 0 & (16)
 \end{aligned}$$

For a time-invariant channel,

$$g_k = 1 \quad k = -K, \dots, K. \quad (17)$$

For a Rayleigh slow-fading channel,

$$g_k \approx g_0 \quad k = -K, \dots K. \quad (18)$$

For the fast-fading channel modeled herein, g_k represents a piecewise constant function; i.e. $g(t)$ is regarded to be effectively constant during the course of each signal pulse, although varying over a long succession of such pulses.

Additive Gaussian Noise

Additive noise due to the channel is modeled by the Gaussian random waveform, $n(t)$, introduced at the filter output. This is equivalent to assuming a Gaussian noise process for the channel because the receiver is modeled as a linear operation and the output of such an operation is Gaussian if and only if its input is Gaussian [17, pp. 474-476]. It is assumed that the noise is zero mean with equal variance σ_n^2 for each bit interval. Thus

$$\begin{aligned} E[n(t)] &= 0 \\ E[n^2(t)] &= \sigma_n^2 \end{aligned} \quad (19)$$

and the density function of the random variable obtained by sampling $n(t)$ is

$$P_{n_k}(\beta_k) = (1/\sigma_n \sqrt{2\pi}) \exp(-\beta_k^2 / 2\sigma_n^2) \quad k = -K, \dots K. \quad (20)$$

Decision Element

As illustrated in Figure 4, the decision element operates on the random variable r_k , which corresponds to message m_k , and which is the k^{th} sampled value of the filter output plus

noise, $r(t)$. The output of the decision element is an estimate, \hat{m}_k , of m_k .

For most systems the probability of error for a single message element is sufficient to characterize the system performance. Hence considering the $k = 0$ sample, the sampled output at $t = \gamma$ may be written

$$r_0 = n(\gamma) + \sum_{k=-K}^K m_k g(kT) h(\gamma - kT). \quad (21)$$

The summation in (21) is limited to $2K+1$ terms on the previous assumption that pulses separated from the zeroth pulse by an interval in excess of KT are greatly attenuated and do not contribute significantly to the intersymbol interference. The behavior of $g(kT)$ has been assumed to be piecewise constant.

In order to simplify the notation, R will be used in place of r_0 , h_k in place of $h(\gamma - kT)$, g_k in place of $g(kT)$ and n in place of $n(\gamma)$. Then (21) can be written

$$R = N + m_0 g_0 h_0 + \sum'_{k=-K}^K m_k g_k h_k \quad (22)$$

where the prime on the summation indicates that the term $k=0$ is to be excluded from the sum. In (22), N is the sampled value of the noise, the middle term is the channel response to the main pulse to be detected and the last term is the intersymbol interference. Define

$$Z = \sum'_{k=-K}^K m_k g_k h_k. \quad (23)$$

Then (22) can be written as

$$R = N + m_0 g_0 h_0 + Z. \quad (24)$$

The total interference is therefore

$$X = N + Z. \quad (25)$$

This is the sampled value of the total distortion mentioned previously. Then (24) can be written as

$$R = m_0 g_0 h_0 + X. \quad (26)$$

For uncorrelated inputs the optimum decision element is a fixed level threshold detector set at the mean of the additive noise. This follows from the well-known result for channels without intersymbol interference [8, pp. 214-219]. Since with an uncorrelated input sequence as assumed in (9), the intersymbol interference will itself be symmetrically distributed about zero, there is no loss of generality to assume

$$h_0 > 0. \quad (27)$$

The decision logic for the zeroth message is then

$$\begin{aligned} R_0 \geq 0 &\longrightarrow \hat{m}_0 = 1, \\ R_0 < 0 &\longrightarrow \hat{m}_0 = -1. \end{aligned} \quad (28)$$

Decision error occurs if R_0 is negative while $m_0=1$, or if R_0 is non-negative while $m_0=-1$.

The Conditional Bit - Error Probability

The probability of error given the value of g_0 can

then be expressed in terms of the relative amplitude of h_0 and X . Thus, making use of (9) and the fact that $n(t)$ is symmetric about a zero mean yields

$$\begin{aligned}
 P[\varepsilon | g_0 = \beta_0] &= P[\varepsilon | \beta_0] \\
 &= \Pr(R \geq 0 | m_0 = -1) \Pr(m_0 = -1) \\
 &\quad + \Pr(R < 0 | m_0 = 1) \Pr(m_0 = 1) \\
 &= \Pr(X \geq \beta_0 h_0 | m_0 = -1) \Pr(m_0 = -1) \\
 &\quad + \Pr(X < -\beta_0 h_0 | m_0 = 1) \Pr(m_0 = 1) \\
 &= 0.5 \Pr(|X| > \beta_0 h_0). \tag{29}
 \end{aligned}$$

Note that $\Pr(|X| = \beta_0 h_0) = 0$ and so this case is excluded.

In terms of $P_X(\beta)$, the density function of the random variable X , equation (29) may be written as

$$P[\varepsilon | g_0 = \beta_0] = \frac{1}{2} - \frac{1}{2} \int_{-\beta_0 h_0}^{\beta_0 h_0} P_X(\beta) d\beta. \tag{30}$$

The density function of a random variable is the Fourier transform of its characteristic function [17, p. 155]. For the example considered herein, it will be shown that $M_X(\lambda)$, the characteristic function of X , is an even function. Thus

$$P_X(\beta) = \frac{1}{2\pi} \int_{-\infty}^{\infty} M_X(\lambda) \cos(\lambda\beta) d\lambda$$

and (30) becomes

$$P[\varepsilon | g_0 = \beta_0] = \frac{1}{2} - \int_{-\beta_0 h_0}^{\beta_0 h_0} \frac{1}{4\pi} \int_{-\infty}^{\infty} M_X(\lambda) \cos(\lambda\beta) d\lambda d\beta.$$

Interchanging the order of integration, and integrating over β yields

$$P[\epsilon | g_0 = \beta_0] = \frac{1}{2} - \frac{1}{\pi} \int_0^{\infty} \frac{\sin(\lambda \beta_0 h_0)}{\lambda} M_X(\lambda) d\lambda \quad (31)$$

where the range of integration has been reduced since the integrand is an even function of λ . This provides $P[\epsilon | \beta_0]$ in terms of the characteristic function of the total distortion X .

The characteristic function of the additive Gaussian noise alone is also an even function, (31) may be written as

$$P[\epsilon | \beta_0] = \frac{1}{2} - \frac{1}{\pi} \int_0^{\infty} \frac{\sin(\lambda \beta_0 h_0)}{\lambda} M_N(\lambda) d\lambda + \frac{1}{\pi} \int_0^{\infty} \frac{\sin(\lambda \beta_0 h_0)}{\lambda} [M_N(\lambda) - M_X(\lambda)] d\lambda \quad (32)$$

The first two terms in this equation are independent of the intersymbol interference. On the other hand, in the absence of intersymbol interference, $Z = 0$ and $X = N$, thus $M_N(\lambda)$ is equivalent to $M_X(\lambda)$ and the third term vanishes. So it is clear that the probability of error given g_0 caused by additive Gaussian noise alone is

$$P_0[\epsilon | \beta_0] = \frac{1}{2} - \frac{1}{\pi} \int_0^{\infty} \frac{\sin(\lambda \beta_0 h_0)}{\lambda} M_N(\lambda) d\lambda, \quad (33)$$

the probability of bit error given β_0 due to intersymbol interference alone is

$$P_Z[\epsilon | \beta_0] = \frac{1}{\pi} \int_0^{\infty} \frac{\sin(\lambda \beta_0 h_0)}{\lambda} [M_N(\lambda) - M_X(\lambda)] d\lambda \quad (34)$$

and

$$P[\epsilon | \beta_0] = P_0[\epsilon | \beta_0] + P_Z[\epsilon | \beta_0]. \quad (35)$$

As will be seen in the next chapter, these expressions

are not so formidable as they might seem at first glance.

Signal - to - Noise Ratio

For a specific fading channel, the mean signal-to-noise ratio, ρ , referred to herein is defined as the ratio of the mean sampled signal power to the RMS noise power. For the purpose of this definition, it is assumed that the signal sample is taken at the optimum sampling instant, $\gamma = 0$. Thus

$$\rho = h^2(0)\mu^2/\sigma_n^2.$$

Making use of assumptions (10) and (15) yields

$$\rho = 1 / \sigma_n^2. \quad (36)$$

Or, as it is customarily expressed in decibels,

$$\rho = -20 \log_{10}(\sigma_n) \text{ dB}. \quad (37)$$

CHAPTER IV

NUMERICAL DETERMINATION OF BIT-ERROR PROBABILITY FOR THE RAYLEIGH FAST-FADING CHANNEL

For Rayleigh fast-fading channels,

$$\begin{aligned} R &= r_0, \\ N &= n, \\ Z &= \sum_{k=-K}^K m_k g_k h_k \end{aligned} \tag{38}$$

Characteristic Function of the Additive Noise

The random variable n is a sample from the Gaussian process $n(t)$. Thus it is a Gaussian random variable with density function as in (20) and has the familiar Gaussian characteristic function [17, pp. 159-160],

$$M_N(\lambda) = \exp(-\lambda^2 \sigma_n^2 / 2). \tag{39}$$

Note that $M_N(\lambda)$ is an even function of λ .

Characteristic Function of the Intersymbol Interference

The density function of the intersymbol interference is rather difficult to determine. However, the characteristic function of the intersymbol interference given g_0 , $M_Z|_{g_0=\beta_0}(\lambda)$, can be obtained as follows.

The definition of the characteristic function of a random variable X is

$$M_X(v) = E[e^{jvX}] = \int_{-\infty}^{\infty} f_X(x) e^{jvx} dx, \tag{40}$$

where $f_X(X)$ is the probability density function of X .

It is also known that the characteristic function of a sum of independent random variables is equal to the product of their individual characteristic functions [17, pp. 213-214]. Now define

$$Z_k = m_k g_k h_k,$$

$$L_k = m_k h_k.$$

Then (38) becomes

$$Z = \sum_{k=-K}^K Z_k = \sum_{k=-K}^K g_k L_k$$

and

$$M_{Z|\beta_0}(\lambda) = M_Z(\lambda) = \prod_{k=-K}^K M_{Z_k}(\lambda) = \prod_{k=-K}^K M_{g_k L_k}. \quad (41)$$

Note that Z is independent of g_0 .

With reference to assumptions in (9), the density function of the random variable L_k is clearly

$$P_{L_k}(\beta) = 0.5\delta(\beta+h_k) + 0.5\delta(\beta-h_k). \quad (42)$$

With reference to (16), the density function of random variable g_k is

$$\begin{aligned} P_{g_k}(\beta_k) &= 0, & \beta_k &< 0 \\ & & k &= -K, \dots, K. \\ &= 2\beta_k \exp(-\beta_k^2), & \beta_k &\geq 0 \end{aligned}$$

The density function of Z_k is the joint density function

of L_k and the density function of g_k ; i.e.

$$P_{Z_k} = P_{L_k} g_k.$$

It is evident that L_k assumes only two values : h_k or $-h_k$.

Once it is determined, Z_k becomes a constant multiple of g_k .

Thus

$$P_{Z_k}(w_k) = \left| \frac{w_k}{h_k^2} \right| \exp\left(-\frac{w_k^2}{h_k^2}\right), \quad w_k \geq 0. \quad (43)$$

Note that it is an even function of w_k . Evidently

$$\begin{aligned} P_{Z_k}(w_k) &\geq 0, \\ \int_{-\infty}^{\infty} P_{Z_k}(w_k) dw_k &= 1. \end{aligned} \quad (44)$$

The expected value of any function of Z_k can be defined in terms of this density function [17, pp. 138-139]. Thus

$$\begin{aligned} M_{Z_k}(\lambda) &= E [\exp(j\lambda w_k)] \\ &= \int_{-\infty}^{\infty} \exp(j\lambda w_k) P_{Z_k}(w_k) dw_k \\ &= \int_{-\infty}^{\infty} \left| \frac{w_k}{h_k^2} \right| \exp\left(-\frac{w_k^2}{h_k^2}\right) \exp(j\lambda w_k) dw_k \\ &= \frac{2}{h_k^2} \int_0^{\infty} w_k \exp\left(-\frac{w_k^2}{h_k^2}\right) \cos \lambda w_k dw_k. \end{aligned} \quad (45)$$

The above follows because $P_{Z_k}(w_k)$ is an even function of w_k .

This integral can be evaluated by referring to a table of definite integrals [18, p. 175], yielding

$$M_{Z_k}(\lambda) = \sum_{n=0}^{\infty} \frac{(-1)^n n!}{(2n+1)!} (\lambda h_k)^{2n}. \quad (46)$$

Combining this result with (41) provides the expression

$$\begin{aligned} M_Z(\lambda) &= \prod_{k=-K}^K M_{Z_k}(\lambda) \\ &= \prod_{k=-K}^K \sum_{n=0}^{\infty} \frac{(-1)^n n!}{(2n+1)!} (\lambda h_k)^{2n}. \end{aligned} \quad (47)$$

Note this is also an even function of λ .

Characteristic Function of the Total Distortion

There is no statistical relation between N and Z ; N and Z are statistically independent. Consequently the characteristic function of the random variable $X = N + Z$ must be

$$\begin{aligned} M_X(\lambda) &= M_N(\lambda) M_Z(\lambda) \\ &= \exp(-\lambda^2 \sigma_n^2 / 2) \prod_{k=-K}^K \sum_{n=0}^{\infty} \frac{(-1)^n n!}{(2n+1)!} (\lambda h_k)^{2n}. \end{aligned} \quad (48)$$

Thus $M_X(\lambda)$ is also an even function of λ . As noted earlier, this is a necessary condition for (31) to hold.

Integral Equation for the Conditional

Bit-Error Probability

Equation (31) can be written in terms of the characteristic function of N and Z ,

$$P[\epsilon | g_0 = \beta_0] = \frac{1}{2} - \frac{1}{\pi} \int_0^{\infty} \frac{\sin(\lambda \beta_0 h_0)}{\lambda} \left[\prod_{k=-K}^K \sum_{n=0}^{\infty} \frac{(-1)^n n!}{(2n+1)!} (\lambda h_k)^{2n} \right] \exp(-\lambda^2 \sigma_n^2 / 2) d\lambda, \quad (49)$$

for the Rayleigh fast-fading channel.

The integral in (49) can be evaluated by expanding the integrand in a power series [2], [3]. The computational efficiency of this sort of approach relies on the existence of recurrence relations for successive terms in the expansions. Such an approach is not satisfactory for this study because the known recurrence relations for the series expansions no longer apply.

The Small Difference Problem

The most straightforward approach to evaluating (49) using a high-speed digital computer is to use a numerical scheme of some sort. If this is to be accomplished, one must overcome the problem that in (49), $P[\epsilon|\beta_0]$ is expressed as a small difference between two relatively large numbers. The slightest error in evaluating the integral drastically affects the result for $P[\epsilon|\beta_0]$.

Fortunately, the problem described above can be circumvented by using the equivalent expression (33), (34) and (35) in place of (31). Then

$$P_0[\epsilon|\beta_0] = \frac{1}{2} - \frac{1}{\pi} \int_0^{\infty} \frac{\sin(\lambda\beta_0 h_0)}{\lambda} \exp(-\lambda^2 \sigma_n^2 / 2) d\lambda \quad (50)$$

$$P_Z[\epsilon|\beta_0] = \frac{1}{\pi} \int_0^{\infty} \frac{\sin(\lambda\beta_0 h_0)}{\lambda} \left[1 - \prod_{k=-K}^K \sum_{n=0}^{\infty} \frac{(-1)^n n!}{(2n+1)!} (\lambda h_k)^{2n} \right] \exp(-\lambda^2 \sigma_n^2 / 2) d\lambda. \quad (51)$$

With regard to (50), reference to a table of definite integrals [19,p.495], yields the relation

$$\frac{2}{\pi} \int_0^{\infty} \frac{\sin(ay)}{y} \exp(-y^2) dy = \text{erf}(a/2)$$

where $\text{erf}(w)$ is the error function, defined by

$$0 \leq \text{erf}(w) = \frac{2}{\sqrt{\pi}} \int_0^w \exp(-\xi^2) d\xi \leq 1.$$

Substituting in (50) as follows,

$$y = \sigma_n / \sqrt{2}$$

$$a = \beta_0 h_0 \sqrt{2} / \sigma_n$$

gives the result

$$\begin{aligned} P_0[\varepsilon | \beta_0] &= 0.5 [1 - \text{erf}(\beta_0 h_0 / \sigma_n \sqrt{2})] \\ &= 0.5 \text{erfc}(\beta_0 h_0 / \sigma_n \sqrt{2}), \end{aligned} \quad (52)$$

where $\text{erfc}(w) = 1 - \text{erf}(w)$ is the complementary error function. Combining (51) and (52) yields

$$\begin{aligned} P[\varepsilon | \beta_0] &= \frac{1}{2} \text{erfc}\left(\frac{\beta_0 h_0}{\sigma_n \sqrt{2}}\right) + \frac{1}{\pi} \int_0^{\infty} \frac{\sin(\lambda \beta_0 h_0)}{\lambda} \\ &\quad \left[1 - \sum_{k=-K}^K \sum_{n=0}^{\infty} \frac{(-1)^n n!}{(2n+1)!} (\lambda h_k)^{2n} \right] \exp(-\lambda^2 \sigma_n^2 / 2) d\lambda. \end{aligned} \quad (53)$$

Integral Equation for the Total Bit-Error Probability

The above expression for bit-error rate in (53) is derived on condition that g_0 is known. Actually g_0 is a random variable of Rayleigh distribution. To obtain the total bit-error rate of the fading channel, it is appropriate to average the conditional bit-error rate over the ensemble of values of g_0 . Thus,

$$\begin{aligned}
P_{e_0} &= \int_0^{\infty} 2\beta_0 e^{-\beta_0^2} P_0[\epsilon|\beta_0] d\beta_0 \\
&= \int_0^{\infty} \beta_0 e^{-\beta_0^2} \operatorname{erfc}(\beta_0 h_0 / \sqrt{2}\sigma_n) d\beta_0.
\end{aligned} \tag{54}$$

It is convenient to define

$$\gamma = g_0^2 / \sigma_n^2,$$

$$\gamma_0 = E[\gamma] = E[g_0^2] / \sigma_n^2 = 1 / \sigma_n^2.$$

Note that the RMS amplitude of $g_0(t)$ is assumed to be 1.

Substituting into (54) yields

$$P_{e_0} = \frac{1}{2} \int_0^{\infty} \frac{1}{\gamma_0} \exp\left(-\frac{\gamma}{\gamma_0}\right) \operatorname{erfc}(h_0 \sqrt{\gamma/2}) d\gamma.$$

Reference to a table of definite integral [19, p. 649] gives

$$P_{e_0} = \frac{1}{2} \left(1 - \frac{1}{\sqrt{1 + 2\sigma_n^2/h_0^2}} \right). \tag{55}$$

Another approach which will lead to the same result is shown below.

$$P_{e_0} = \int_0^{\infty} 2\beta_0 e^{-\beta_0^2} P_0[\epsilon|\beta_0] d\beta_0. \tag{56}$$

Substituting (50) into (56) gives

$$\begin{aligned}
P_{e_0} &= \int_0^{\infty} 2\beta_0 e^{-\beta_0^2} \left[\frac{1}{2} - \frac{1}{\pi} \int_0^{\infty} \frac{\sin(\lambda \beta_0 h_0)}{\lambda} \exp(-\lambda^2 \sigma_n^2/2) d\lambda \right] d\beta_0 \\
&= \frac{1}{2} - \frac{1}{\pi} \int_0^{\infty} 2\beta_0 e^{-\beta_0^2} \int_0^{\infty} \frac{\sin(\lambda \beta_0 h_0)}{\lambda} \exp(-\lambda^2 \sigma_n^2/2) d\lambda d\beta_0.
\end{aligned} \tag{57}$$

Interchanging the order of integration, and integrating over β_0 using a reference to a table of integrals [20, p. 236] yields

$$P_{e_0} = \frac{1}{2} - \frac{h_0}{2\sqrt{\pi}} \int_0^{\infty} \exp(-h_0^2 \lambda^2 / 4 - \sigma_n^2 \lambda^2 / 2) d\lambda. \quad (58)$$

Again, reference to a table of definite integrals [20, p. 230] gives the result

$$P_{e_0} = \frac{1}{2} \left(1 - \frac{1}{\sqrt{1 + 2\sigma_n^2 / h_0^2}} \right). \quad (59)$$

This is the average bit-error rate due to additive Gaussian noise alone.

The same method also applies to calculating the bit-error rate due to intersymbol interference, P_{e_z} .

$$P_{e_z} = \int_0^{\infty} 2\beta_0 e^{-\beta_0^2} P_z[\varepsilon | \beta_0] d\beta_0. \quad (60)$$

Substituting (51) into (60) gives

$$P_{e_z} = \int_0^{\infty} 2\beta_0 e^{-\beta_0^2} \frac{1}{\pi} \frac{\sin(\lambda \beta_0 h_0)}{\lambda} \left[1 - \prod_{k=-K}^K \sum_{n=0}^{\infty} \frac{(-1)^n n!}{(2n+1)!} (\lambda h_k)^{2n} \right] \exp(-\lambda^2 \sigma_n^2 / 2) d\beta_0 d\lambda. \quad (61)$$

Interchanging the order of integration and integrating over β_0 using reference to a table of definite integrals [20, p. 236] yields the relation

$$P_{e_z} = \frac{h_0}{2\sqrt{\pi}} \int_0^{\infty} \left[1 - \prod_{k=-K}^K \sum_{n=0}^{\infty} \frac{(-1)^n n!}{(2n+1)!} (\lambda h_k)^{2n} \right] \exp(-h_0^2 \lambda^2 / 4 - \sigma_n^2 \lambda^2 / 2) d\lambda. \quad (62)$$

Combining (59) and (62) yields

$$P_e = \frac{1}{2} \left(1 - \frac{1}{\sqrt{1 + 2\sigma_n^2 / h_0^2}} \right) + \frac{h_0}{2\sqrt{\pi}} \int_0^{\infty} \left[1 - \prod_{k=-K}^K \sum_{n=0}^{\infty} \frac{(-1)^n n!}{(2n+1)!} (\lambda h_k)^{2n} \right] \exp(-h_0^2 \lambda^2 / 4 - \sigma_n^2 \lambda^2 / 2) d\lambda. \quad (63)$$

This last equation is much better suited for numerical integration because the integrand is now everywhere much smaller relative to P_e and because P_e is now expressed as the sum of two small positive terms. In fact, the "small difference of two relatively large quantities" has been moved into the integrand of (63).

Truncation Error

In order to make numerical integration practical, the infinite integral in (63) must converge in such a fashion that it can be truncated at some relatively small upper limit without introducing excessive error. Call this limit A and let the truncation error be designated E_T . Then

$$P_e = P_{e_0} + E_T + \frac{h_0}{2\sqrt{\pi}} \int_0^A \left[1 - \prod_{k=-K}^K \sum_{n=0}^{\infty} \frac{(-1)^n n!}{(2n+1)!} (\lambda h_k)^{2n} \right] \exp(-h_0^2 \lambda^2 / 4 - \sigma_n^2 \lambda^2 / 2) d\lambda, \quad (64)$$

and

$$E_T = \frac{h_0}{2\sqrt{\pi}} \int_A^{\infty} \left[1 - \prod_{k=-K}^K \sum_{n=0}^{\infty} \frac{(-1)^n n!}{(2n+1)!} (\lambda h_k)^{2n} \right] \exp(-h_0^2 \lambda^2 / 4 - \sigma_n^2 \lambda^2 / 2) d\lambda. \quad (65)$$

In order to obtain an easily evaluated upper bound for E_T , observe that the series in the bracket can be represented by a closed-form expression [21, p. 85],

$$\sum_{n=0}^{\infty} \frac{(-1)^n n!}{(2n+1)!} (\lambda h_k)^{2n} = \frac{2}{\lambda h_k} \exp(-h_k^2 \lambda^2 / 4) \operatorname{erfi}(\lambda h_k / 2) \quad (66)$$

where $\operatorname{erfi}(x)$ is the error function with imaginary argument; i.e.

$$\operatorname{erfi}(x) = \int_0^x e^{t^2} dt.$$

Substituting (63) into (60) yields

$$P_e = \frac{1}{2} \left(1 - \frac{1}{\sqrt{1 + 2\sigma_n^2 / h_0^2}} \right) + \frac{h_0}{2\sqrt{\pi}} \int_0^{\infty} \left[1 - \prod_{k=-K}^K \frac{2}{\lambda h_k} \exp(-h_k^2 \lambda^2 / 4) \operatorname{erfi}(\lambda h_k / 2) \right] \exp(-h_0^2 \lambda^2 / 4 - \sigma_n^2 \lambda^2 / 2) d\lambda. \quad (67)$$

Substituting $x = \frac{1}{2} \lambda h_k$ gives the result

$$P_e = \frac{1}{2} \left(1 - \frac{1}{\sqrt{1 + 2\sigma_n^2 / h_0^2}} \right) + \frac{h_0}{2\sqrt{\pi}} \int_0^{\infty} \left[1 - \prod_{k=-K}^K \left(\frac{1}{x} e^{-x^2} \int_0^x e^{t^2} dt \right) \right] \exp(-h_0^2 \lambda^2 / 4 - \sigma_n^2 \lambda^2 / 2) d\lambda. \quad (68)$$

The factor inside the parenthesis is in the familiar form of Dawson Integral divided by x . Reference to a table of Dawson

Integral [22], [23] yields the relations,

$$0 \leq \frac{K}{\pi} \frac{1}{x} e^{-x^2} \int_0^x e^{t^2} dt \leq 1. \quad (69)$$

Thus

$$E_T \leq \frac{h_0}{2\sqrt{\pi}} \exp(-h_0^2 \lambda^2 / 4 - \sigma_n^2 \lambda^2 / 2) d\lambda, \quad (70)$$

which can be expressed in terms of the complementary error function by substituting in (67) as follows ,

$$y = \sqrt{\frac{h_0^2}{4} + \frac{\sigma_n^2}{2}}.$$

Then the result is

$$E_T \leq \frac{h_0}{4 \sqrt{\frac{h_0^2}{4} + \frac{\sigma_n^2}{2}}} \operatorname{erfc}\left(A \sqrt{\frac{h_0^2}{4} + \frac{\sigma_n^2}{2}}\right). \quad (71)$$

Since $\operatorname{erfc}(w)$ is well tabulated. E_T can be upper-bounded easily enough from (71). Or conversely, if a maximum tolerable truncation error is known, then a minimum value can be found for the upper limit of integration, A .

Although the closed-form expression (66) looks easier to evaluate, it will be necessary to approximate the function $\operatorname{erfi}(x)$ by a power series expansion which leaves the expression for bit-error probability no simpler than (64). The computer time required to execute the calculation is expected to be the same. Thus, (64) is used to calculate the result.

The formula for integration between 0 and A using the elementary trapezoidal rule is

$$\int_0^A f(y) dy \approx \frac{\Delta}{2} [f(0) + f(A)] + \Delta \sum_{j=1}^J f(j\Delta) \quad (72)$$

where

$$\Delta = A/J.$$

If A and J are made to tend to infinity in such a manner that Δ remains fixed, (72) becomes [24]

$$\int_0^{\infty} f(y) dy = \frac{\Delta}{2} f(0) + \Delta \sum_{j=1}^{\infty} f(j\Delta) + \epsilon_T \quad (73)$$

where

$$\epsilon_T = -2 \sum_{j=1}^{\infty} F(2j\pi/\Delta),$$

and

$$F(w) = \int_0^{\infty} f(y) \cos(wy) dy.$$

If $f(y)$ is an even function such that the error term becomes negligibly small, the trapezoidal integration rule may be used with arbitrarily small errors [25].

Determination of Terms Used in the Series Expansion

The series in the bracket of (65) for calculating P_{e_z} decreases very rapidly as n increases.

Convergence tests were run using different values of n ($n = 1$ to $n = 10$). The results show that $n = 3$ provides in excess of seven significant digits accuracy for P_{e_z} for both Gaussian and Chebyshev pulses.

Magnitude of Integration Error

A direct evaluation of the Fourier coefficients in (73) is difficult, if not impossible. Therefore, in order to determine a suitable value for Δ in the trapezoidal integration rule, the digital computer program was modified to allow calculation of P_{e_z} for a given data point using a range of values for Δ .

Convergence tests were run using this modified program. The results are presented in Table 1 for the Gaussian pulse with $K = 2$, $\gamma = 0$ to $0.4T$, and with signal-to-noise ratios ranging from 0 dB to 35 dB. Similar data are shown in Table 2 for the Chebyshev pulse with $K = 20$, $\gamma = 0$ to $0.2T$ and with the same range of signal-to-noise ratios. In all cases, Δ was varied between 0.6 and 3.0 in steps of 0.2. The upper limit of integration, A , was selected to keep E_T less than 10^{-14} for all data points.

Interpretation of data in Tables 1 and 2 shows that a choice of $\Delta = 1.2$ assures convergence to within 0.02 of the correct values for P_{e_z} at all signal-to-noise ratios. The worst cases are seen to occur at very low signal-to-noise ratios which are probably not of much practical interest. In the middle range of signal-to-noise ratios, $\Delta = 1.2$ typically provides in excess of six significant digit accuracy.

The Bit-Error Probabilities for the Rayleigh Fast-Fading Channel

In order to systematically determine P_e , P_{e_0} and P_{e_z}

Table 1. Convergence of Numerical Integration for the
Rayleigh Fast-Fading Channel, Gaussian Pulse

Step size, Δ	Calculated value for P_{e_z} with $\gamma = 0$		
	$\rho = 0$ dB	$\rho = 15$ dB	$\rho = 30$ dB
3.0	2.2046×10^{-5}	1.7264×10^{-3}	1.9845×10^{-3}
2.8	4.2839×10^{-5}	1.9217×10^{-3}	2.1738×10^{-3}
2.6	7.7193×10^{-5}	2.0737×10^{-3}	2.3146×10^{-3}
2.4	1.2867×10^{-4}	2.1759×10^{-3}	2.4041×10^{-3}
2.2	1.9781×10^{-4}	2.3830×10^{-3}	2.4502×10^{-3}
2.0	2.7942×10^{-4}	2.2555×10^{-3}	2.4678×10^{-3}
1.8	3.6129×10^{-4}	2.2621×10^{-3}	2.4723×10^{-3}
1.6	4.2701×10^{-4}	2.2631×10^{-3}	2.4729×10^{-3}
1.4	4.6484×10^{-4}	2.2632×10^{-3}	2.4729×10^{-3}
1.2	4.7762×10^{-4}	2.2632×10^{-3}	2.4729×10^{-3}
1.0	4.7937×10^{-4}	2.2632×10^{-3}	2.4729×10^{-3}
0.8	4.7942×10^{-4}	2.2632×10^{-3}	2.4729×10^{-3}
0.6	4.7942×10^{-4}	2.2632×10^{-3}	2.4729×10^{-3}

Table 1. (concluded)

Step size, Δ	Calculated value for P_{e_z} with $\gamma = 0.4T$		
	$\rho = 0$ dB	$\rho = 15$ dB	$\rho = 30$ dB
3.0	5.9103×10^{-4}	4.6148×10^{-2}	5.2967×10^{-2}
2.8	9.9616×10^{-4}	4.9619×10^{-2}	5.8522×10^{-2}
2.6	1.5717×10^{-3}	4.9737×10^{-2}	5.8494×10^{-2}
2.4	2.3161×10^{-3}	4.9601×10^{-2}	5.8123×10^{-2}
2.2	3.1787×10^{-3}	4.9058×10^{-2}	5.7111×10^{-2}
2.0	4.0515×10^{-3}	4.7758×10^{-2}	5.5002×10^{-2}
1.8	4.7888×10^{-3}	4.9665×10^{-2}	5.8248×10^{-2}
1.6	5.2699×10^{-3}	4.8995×10^{-2}	5.7039×10^{-2}
1.4	5.4816×10^{-3}	4.9620×10^{-2}	5.8167×10^{-2}
1.2	5.5310×10^{-3}	4.8485×10^{-2}	5.6224×10^{-2}
1.0	5.5350×10^{-3}	4.8645×10^{-2}	5.6493×10^{-2}
0.8	5.5350×10^{-3}	4.9339×10^{-2}	5.7663×10^{-2}
0.6	5.5350×10^{-3}	4.8937×10^{-2}	5.6985×10^{-2}

Table 2. Convergence of Numerical Integration for the Rayleigh Fast-Fading Channel, Chebyshev Pulse

Step size, Δ	Calculated value for P_{e_z} with $\gamma = 0$		
	$\rho = 0$ dB	$\rho = 15$ dB	$\rho = 30$ dB
3.0	1.0100×10^{-5}	7.9099×10^{-4}	9.0926×10^{-4}
2.8	1.9612×10^{-5}	8.7988×10^{-4}	9.9536×10^{-4}
2.6	3.5316×10^{-5}	9.4896×10^{-4}	1.0592×10^{-3}
2.4	5.8833×10^{-5}	9.9528×10^{-4}	1.0998×10^{-3}
2.2	9.0394×10^{-5}	1.0207×10^{-3}	1.1206×10^{-3}
2.0	1.2762×10^{-4}	1.0313×10^{-3}	1.1286×10^{-3}
1.8	1.6494×10^{-4}	1.0342×10^{-3}	1.1305×10^{-3}
1.6	1.9487×10^{-4}	1.0347×10^{-3}	1.1308×10^{-3}
1.4	2.1207×10^{-4}	1.0347×10^{-3}	1.1308×10^{-3}
1.2	2.1788×10^{-4}	1.0347×10^{-3}	1.1308×10^{-3}
1.0	2.1867×10^{-4}	1.0347×10^{-3}	1.1308×10^{-3}
0.8	2.1869×10^{-4}	1.0347×10^{-3}	1.1308×10^{-3}
0.6	2.1869×10^{-4}	1.0347×10^{-3}	1.1308×10^{-3}

Table 2. (concluded)

Step size, Δ	Calculated value for P_{e_z} with $\gamma = 0.2T$		
	$\rho = 0$ dB	$\rho = 15$ dB	$\rho = 30$ dB
3.0	2.0882×10^{-4}	1.6399×10^{-2}	1.8878×10^{-2}
2.8	3.9419×10^{-4}	1.7789×10^{-2}	2.0174×10^{-2}
2.6	6.9142×10^{-4}	1.8791×10^{-2}	2.1059×10^{-2}
2.4	1.1243×10^{-3}	1.9405×10^{-2}	2.1567×10^{-2}
2.2	1.6893×10^{-3}	1.9707×10^{-2}	2.1797×10^{-2}
2.0	2.3372×10^{-3}	1.9817×10^{-2}	2.1873×10^{-2}
1.8	2.9671×10^{-3}	1.9842×10^{-2}	2.1888×10^{-2}
1.6	3.4545×10^{-3}	1.9845×10^{-2}	2.1890×10^{-2}
1.4	2.7222×10^{-3}	1.9846×10^{-2}	2.1890×10^{-2}
1.2	3.8070×10^{-3}	1.9846×10^{-2}	2.1890×10^{-2}
1.0	3.8177×10^{-3}	1.9846×10^{-2}	2.1890×10^{-2}
0.8	3.8179×10^{-3}	1.9846×10^{-2}	2.1890×10^{-2}
0.6	3.8179×10^{-3}	1.9846×10^{-2}	2.1890×10^{-2}

for the Rayleigh fast-fading channel, the digital computer program is written to allow the user to specify the pulse shape and a range of sampling instants and signal-to-noise ratios. Details of this final version of the program are given in Appendix B1.

Plots of P_e and P_{e_z} versus signal-to-noise ratio, as obtained using the program, are shown in Figures 5 - 9 for the Gaussian pulse. Curves for sampling instants of 0, 0.1T, 0.2T, 0.3T and 0.4T are shown individually. Five pulses were used in the approximation of $h(t)$ for these curves; i.e. $K = 2$. For the Gaussian pulse, use of K greater than 2 affected the calculated values for P_{e_z} only after the eighth significant digit. This was determined by running convergence tests for K .

The curves for Figures 5 - 9 were drawn from a total of 70 points. Execution time to compute P_{e_0} , P_{e_z} and P_e for all these points was 15.4 seconds using $\Delta = 0.6$. The limit of integration, A , was selected to hold E_T below 10^{-14} for all cases.

Performance with the Chebyshev pulse was also evaluated. Plots of P_e and P_{e_z} versus signal-to-noise ratio are shown in Figures 10 - 14 for this case. Curves for sampling instants of 0, 0.05T, 0.1T, 0.15T and 0.2T are shown individually. Forty-one pulses were used in the approximation of $h(t)$ for these curves; i.e. $k = 20$. This is determined by running convergence tests for K . For this pulse shape, the use of more pulses affects the values calculated for P_{e_z} only after about

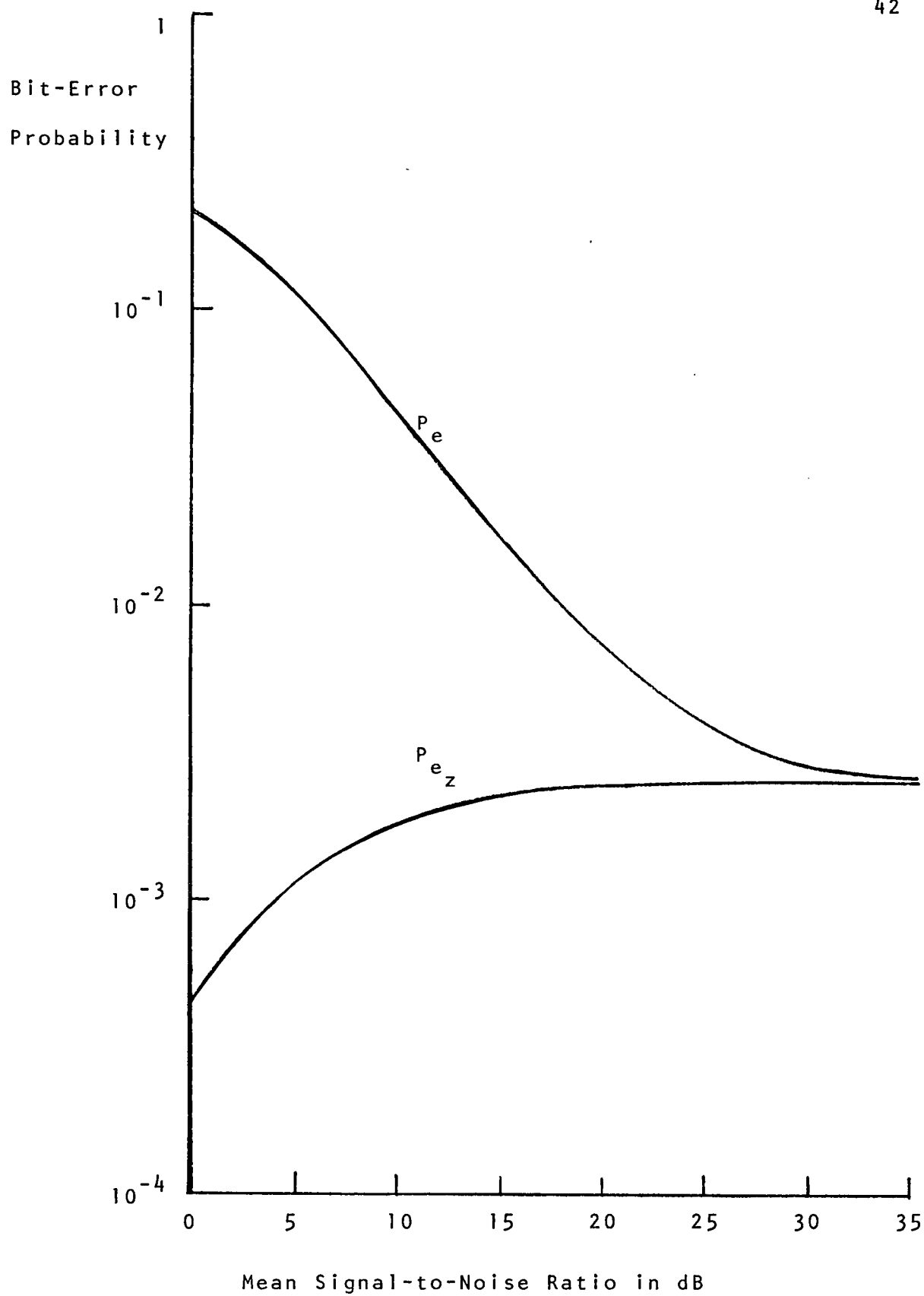


Figure 5. Performance of Rayleigh Fast-Fading Channel:
Gaussian Pulse, $\gamma = 0$

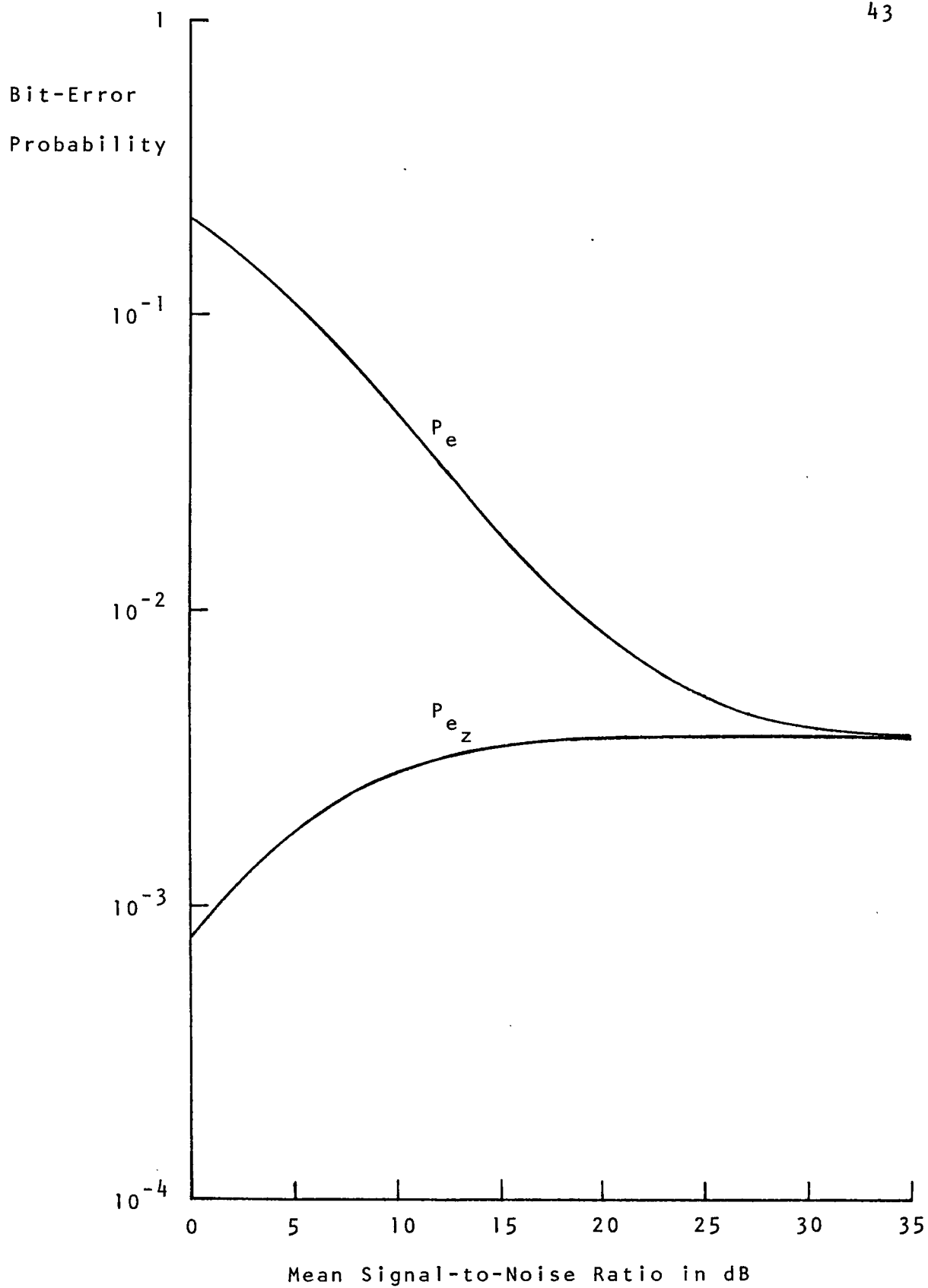


Figure 6. Performance of Rayleigh Fast-Fading Channel:
Gaussian Pulse, $\gamma = 0.1T$

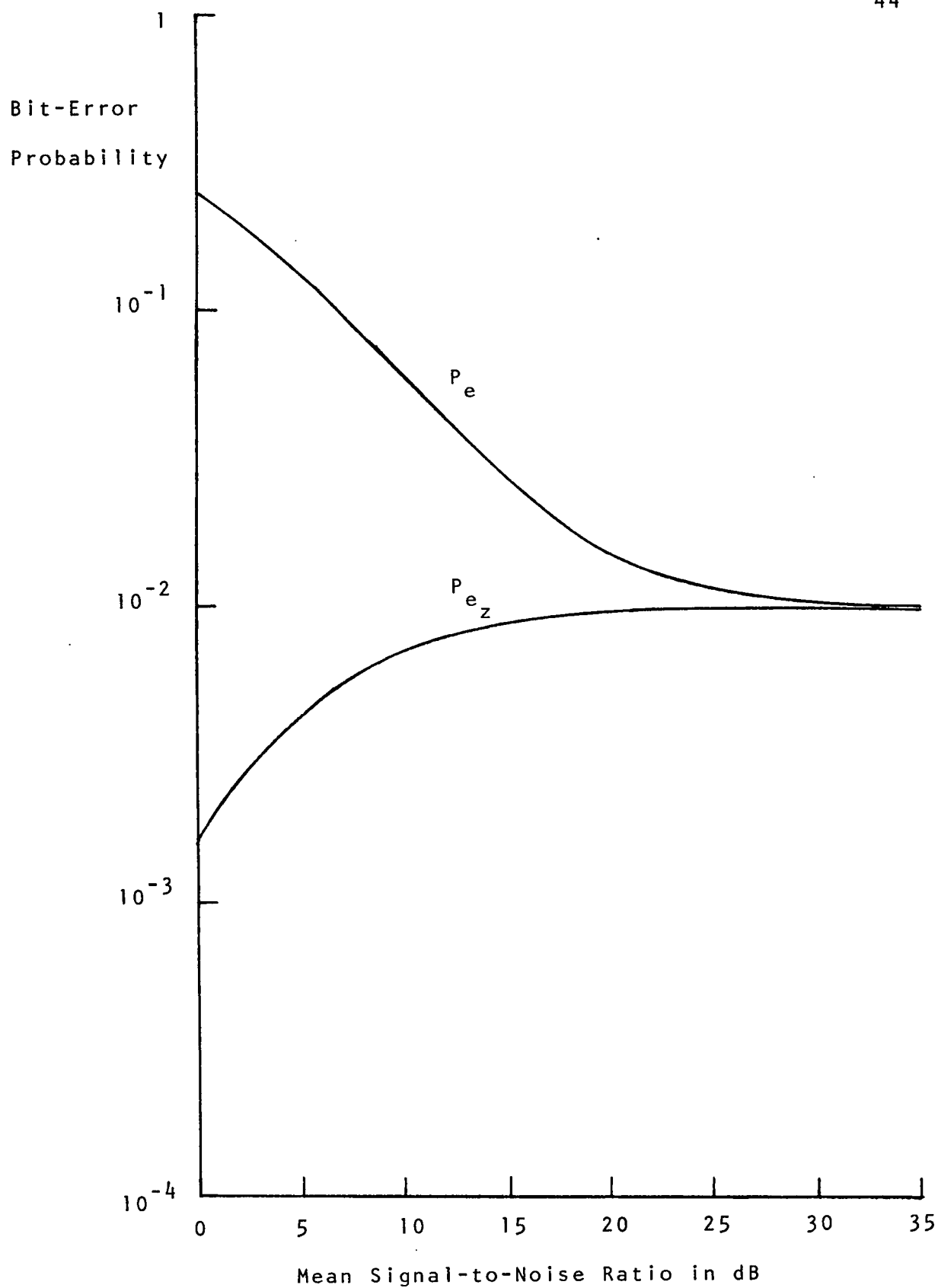


Figure 7. Performance of Rayleigh Fast-Fading Channel:
Gaussian Pulse, $\gamma = 0.2T$

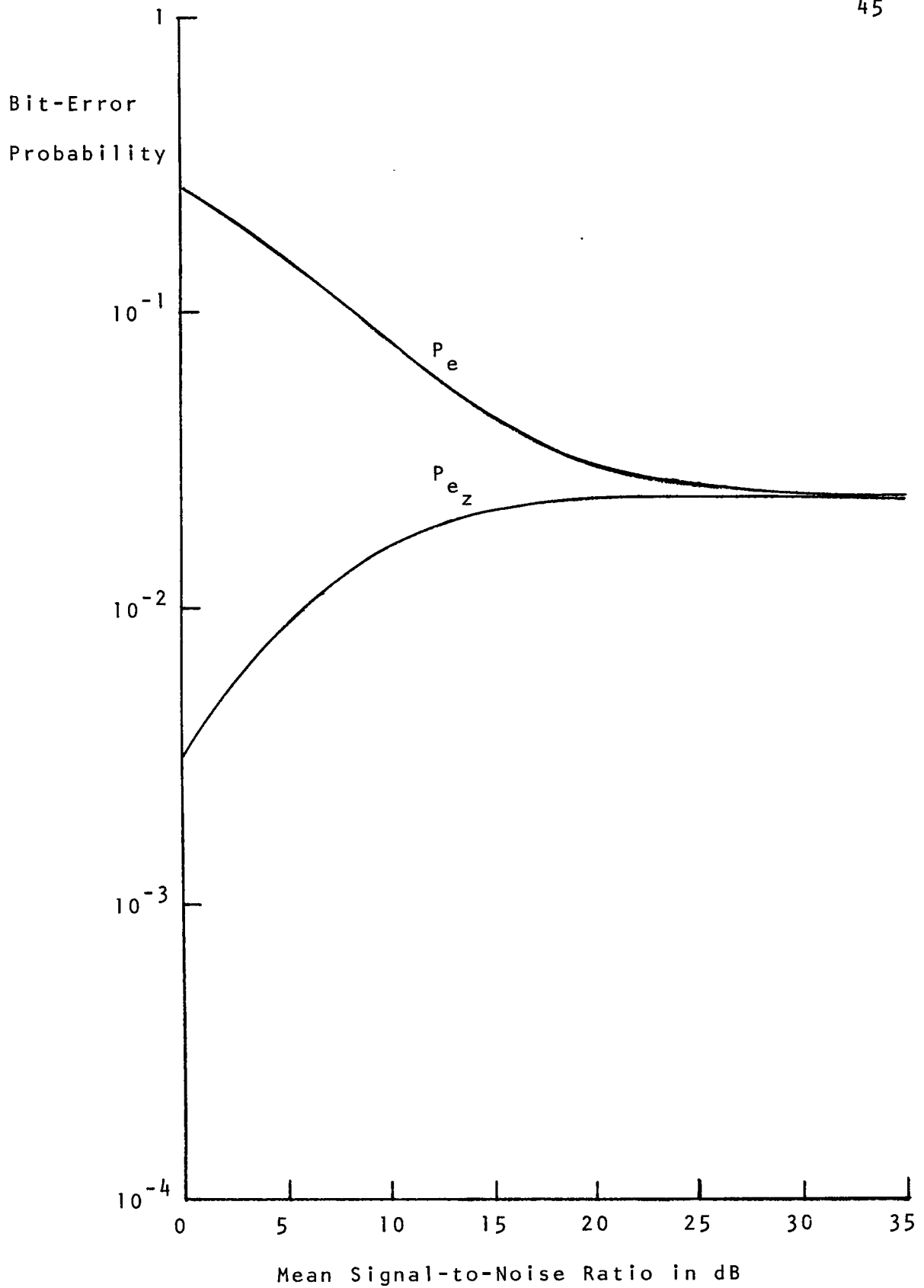


Figure 8. Performance of Rayleigh Fast-Fading Channel:
Gaussian Pulse, $\gamma = 0.3T$

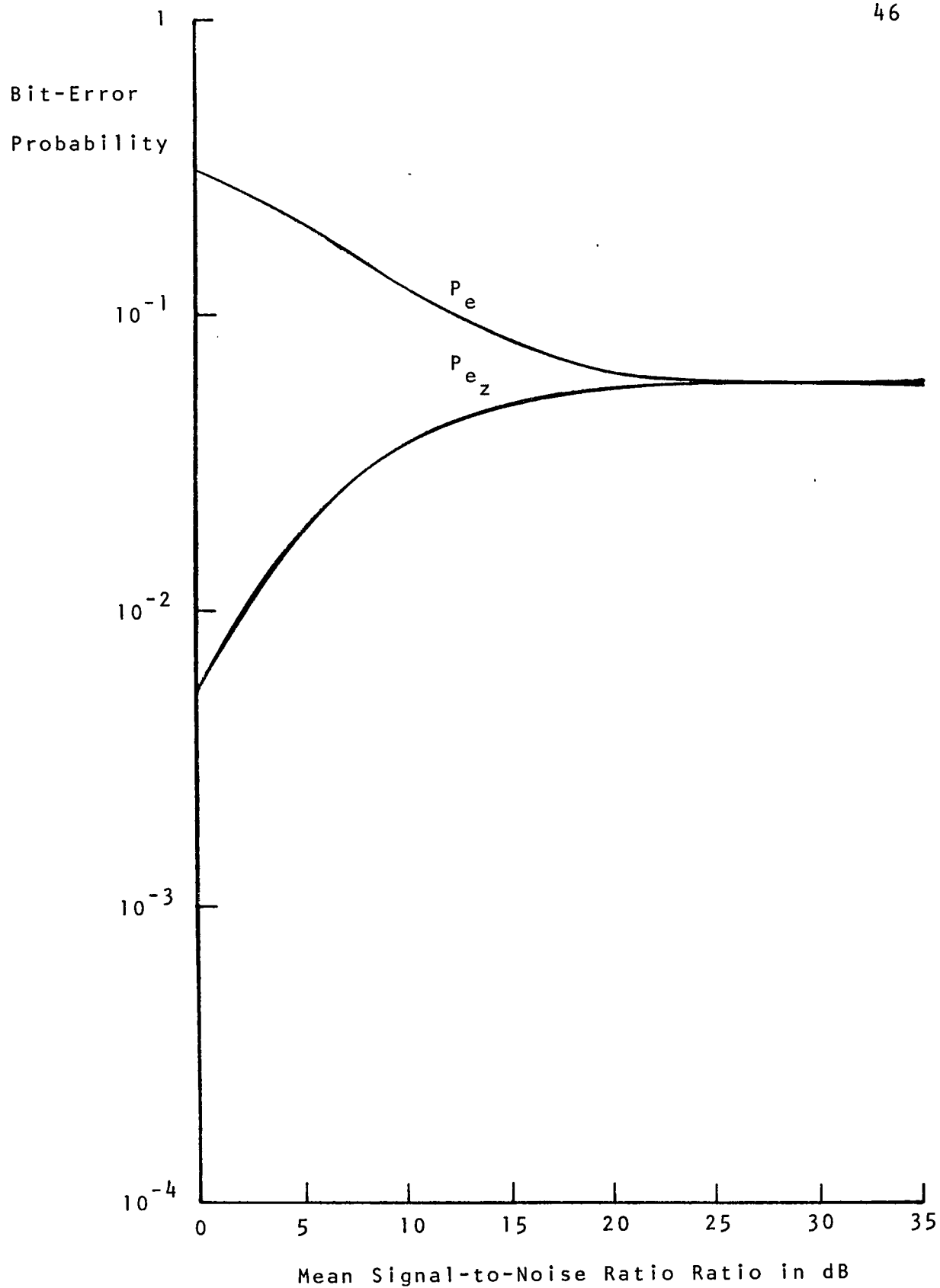


Figure 9. Performance of Rayleigh Fast-Fading Channel:
Gaussian Pulse, $\gamma = 0.4T$

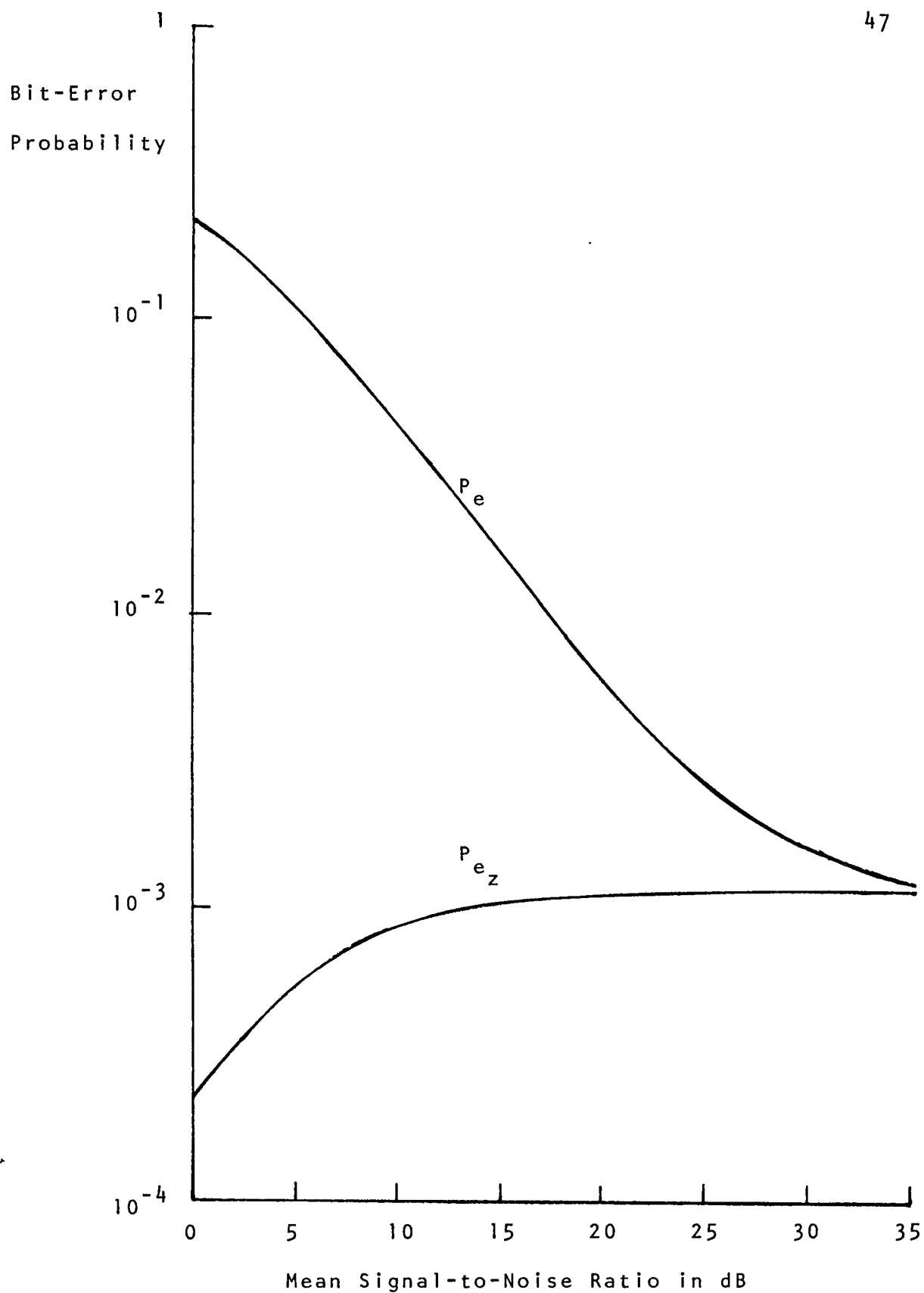


Figure 10. Performance of Rayleigh Fast-Fading Channel:
Chebyshev Pulse, $\gamma = 0$

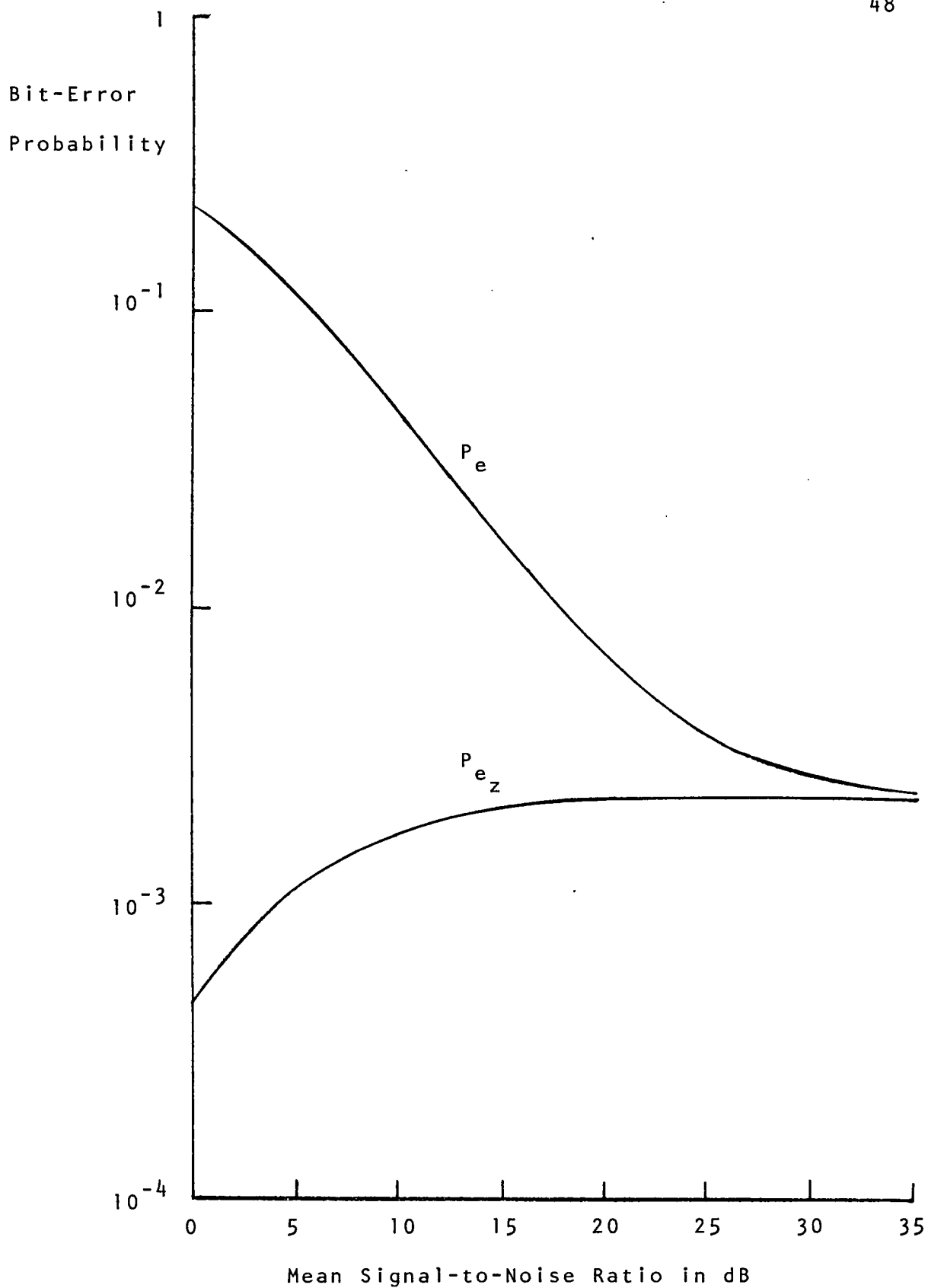


Figure 11. Performance of Rayleigh Fast-Fading Channel:
Chebyshev Pulse, $\gamma = 0.05T$

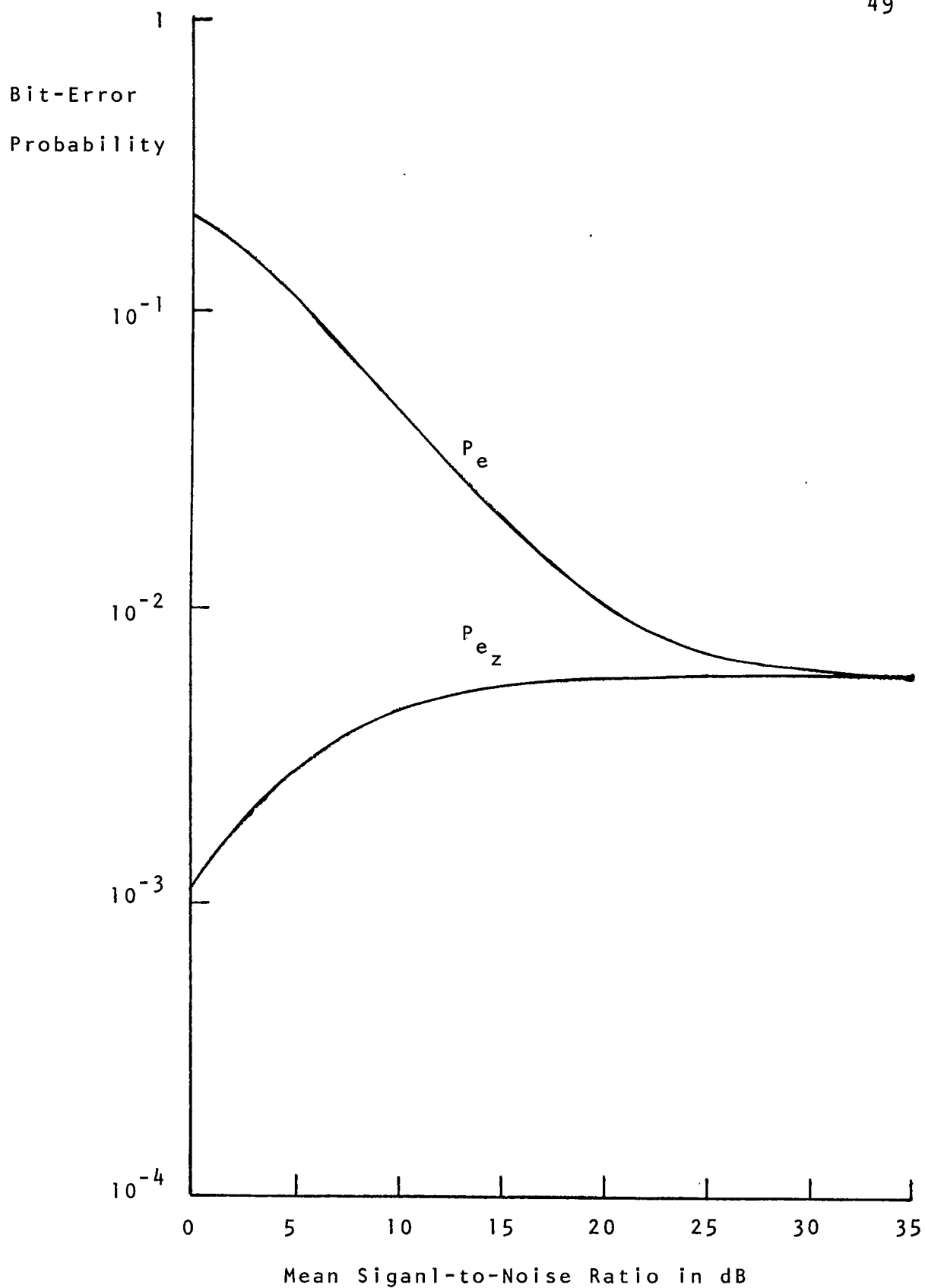


Figure 12. Performance of Rayleigh Fast-Fading Channel:
Chebyshev Pulse, $\gamma = 0.1T$

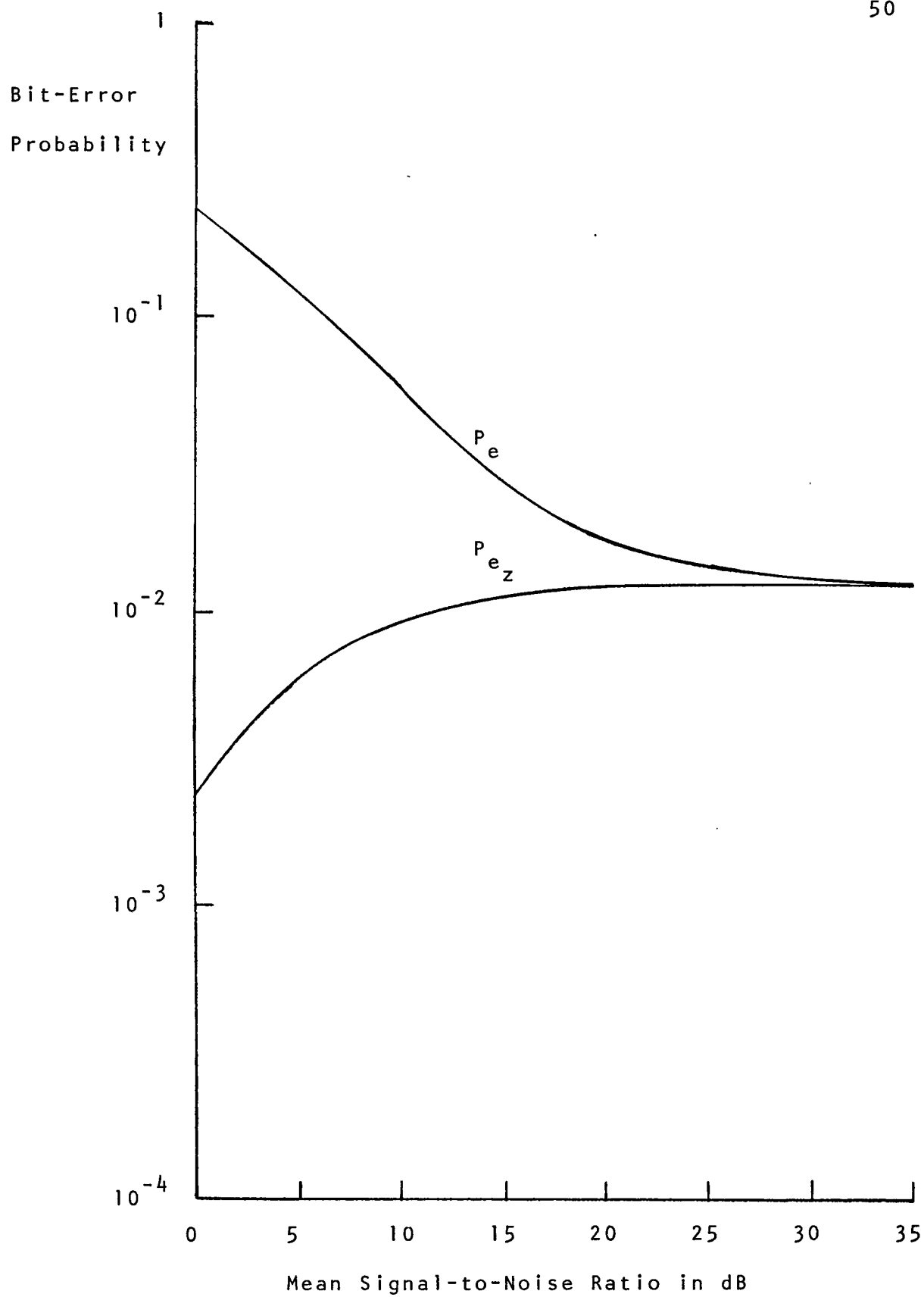


Figure 13. Performance of Rayleigh Fast-Fading Channel:
Chebyshev Pulse, $\gamma = 0.15T$

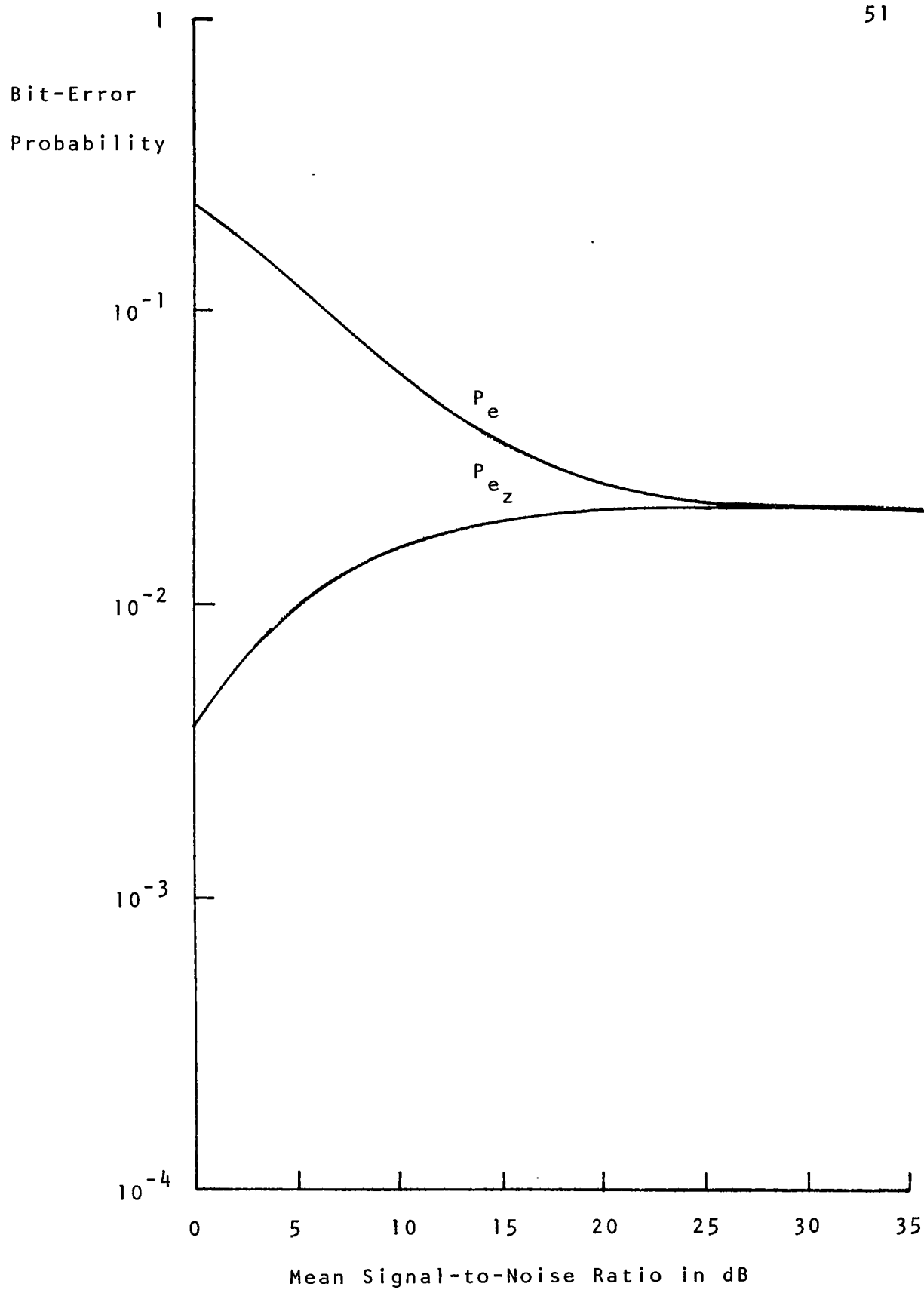


Figure 14. Performance of Rayleigh Fast-Fading Channel:
Chebyshev Pulse, $\gamma = 0.2T$

the seventh significant digits.

This set of curves was also drawn from a total of 70 data points. The execution time was longer, being 17.691 seconds, due primarily to the large value of K . The limit of integration was again chosen to hold E_T at less than 10^{-14} and a step size of 0.6 was used.

Further, it should be noted that the larger sampling instants of $0.2T$ to $0.4T$ for the Gaussian pulses and $0.1T$ to $0.2T$ for the Chebyshev represent operationally poor situations that are not usually encountered in practice.

Asymptotic Behavior of P_{e_z}

In order to study the behavior of P_{e_z} , the series expansion in (62) is approximated by the sum of the first two terms ;i.e. $n = 0$ and $n = 1$. P_{e_z} is then calculated with the Gaussian pulse shape, $K = 1$ and $\gamma = 0$. Reference to a table of definite integrals [20, p. 236] yields the relation

$$P_{e_z} \approx 2.5 \times 10^{-4} \frac{h_0}{(h_0^2/4 + \sigma_n^2/2)^{3/2}} . \quad (74)$$

This expression is not very accurate for practical calculation, but it gives a clear relation between P_{e_z} and σ_n^2 . Combining (36) and (74) yields

$$P_{e_z} \sim \rho^{3/2} ; \quad (75)$$

i.e. P_{e_z} increases with $\rho^{3/2}$ where ρ is the signal-to-noise ratio. This effect will cancel out the inversely decreasing

effect of P_{e_0} with ρ when the signal-to-noise ratio increases to higher level. It is important to note that there is a maximum value for P_{e_z} at $\sigma_n^2 = 0$,

$$P_{e_{z_{\max}}} \approx 2 \times 10^{-3} / h_0^2. \quad (76)$$

Physically this denotes the situation where the signal-to-noise ratio is increased to infinity.

The expression in (76) also designates an irreducible error due to intersymbol interference; i.e. an asymptotic probability of error beyond which the system performance can not be improved no matter how large the mean signal-to-noise ratio becomes.

Note P_{e_z} in Figures 5 - 14 follows the predicted behavior closely; i.e. increases with signal-to-noise ratio to a level (about 25 dB) where an irreducible error is created.

Overall Effects of Intersymbol Interference on Total Bit-Error Probability

It is anticipated that the effects of intersymbol interference on the Rayleigh fast-fading channels will be more significant than those of slow-fading channels. With regard to Figures 5 - 14, when the mean signal-to-noise ratio is below 15 dB, the effects of intersymbol interference are not significant enough to degrade the system performance; but note that for mean signal-to-noise ratios in excess of 15 dB, the fraction of P_{e_z} / P_e increases very rapidly, as also seen

in Table 3; and for mean signal-to-noise ratios in excess of 25 dB, P_{e_z}/P_e approaches 1; i.e. the total bit-error probability is almost entirely due to intersymbol interference. An irreducible error rate is also observed beyond this level. This is well known as the bottoming effect or asymptotic effect [26], [27]. Normally, this effect will occur when the signal-to-noise ratio is 40 dB or more. For Rayleigh fast-fading channels with additive Gaussian noise and intersymbol interference, this effect occurs even at lower levels of signal-to-noise ratio (25 dB or more) to worsen the performance of the system.

Convergence tests run for various K also show that the assumption one only has to take account of the preceding and following waveforms in calculating probability of error due to intersymbol interference for a particular symbol waveform might not be valid for some pulses.

While reliable communications over fading channels requires large mean signal-to-noise ratios or diversity techniques, or both, the data in Table 3 indicates that intersymbol interference becomes a serious problem in Rayleigh fast-fading channels and application of equalization techniques should also be used to combat the system degradation due to intersymbol interference.

Table 3. Asymptotic Behavior of P_{e_z} / P_e

with $\gamma = 0$

Pulse Shape SNR ρ (dB)	Gaussian	Chebyshev
	Pulse, $K = 2$	Pulse, $K = 20$
0	2.2636×10^{-3}	1.0338×10^{-3}
15	1.3035×10^{-1}	6.4136×10^{-2}
25	5.9684×10^{-1}	4.1659×10^{-1}
35	9.4002×10^{-1}	8.7756×10^{-1}
45	9.9367×10^{-1}	9.8626×10^{-1}
55	9.9940×10^{-1}	9.9859×10^{-1}
65	9.9996×10^{-1}	9.9998×10^{-1}
Irreducible Bit- Error Probability	2.4803×10^{-3}	1.1342×10^{-3}

CHAPTER V

CONCLUSION

A very straightforward method has been developed to compute the probability of bit-error for digital communication systems employing coherent detection in the presence of additive Gaussian noise and intersymbol interference. The method is based on the trapezoidal integration rule, and it is applied to Rayleigh fast-fading channel.

By using the above-mentioned computing scheme, the effects of intersymbol interference on typical systems operating over a Rayleigh fast-fading channels are shown to be very significant in most signal-to-noise ratio levels. As the mean signal-to-noise ratio is increased, thereby reducing the total bit-error probability, P_e , the ratio P_{e_z}/P_e increases very rapidly. This behavior is observed in all examples considered herein and empirically derived values for the fraction are tabulated in Chapter IV.

The most important observation of this study is the existence of an irreducible asymptotic bit-error rate due to the severity of intersymbol interference. The dependence of the irreducible error with parameters of intersymbol interference has not been considered, and this could be the subject of further study.

For Rayleigh fast-fading channels, it seems necessary to employ equalization techniques to combat the severe effects of intersymbol interference. The improved performance of

systems utilizing both diversity and equalization is also a very interesting subject of further study.

Numerical results of this study have been compared, where possible, to similar data published by other authors [2], [3], [26], [27]. No point of disagreement was found. Furthermore, the analytic expressions derived in Chapter III and IV for the bit-error probability caused only by additive Gaussian noise are in agreement with well-known results by many authors [15], [16].

REFERENCES

- [1] B. R. Saltzberg, "Intersymbol Interference Error Bounds with Application to Ideal Bandlimited Signalling," IEEE Trans. Inform. Theory, Vol. IT-14, July 1968, pp. 563-568.
- [2] O. Shimbo, M. I. Celebiler, "The Probability of Error due to Intersymbol Interference and Gaussian Noise in Digital Communication Systems," IEEE Trans. Commun. Tech., Vol. COM-19, April 1971, pp. 113-119.
- [3] E. Y. Ho, Y. S. Yeh, "A New Approach for Evaluating the Error Probability in the Presence of Intersymbol Interference and Additive Gaussian Noise," Bell Syst. Tech. J., Vol. 49, Nov. 1970, pp. 2249-2265.
- [4] K. Bullington, W. J. Inkster and A. L. Durkee, "Results of Propagation Tests at 505 mc and 4,090 mc on Beyond-Horizon Paths," Proc. IRE, Vol. 43, Oct. 1955, pp. 1306-1316.
- [5] G. L. Grisdale, et. al. "Fading of Long-Distance Radio Signals and a Comparison of Space and Polarization-Diversity Reception in the 6 - 18 mc/s Range," Proc. Inst. Elec. Eng., Vol. 104, part B, Jan. 1957, pp. 39-51.
- [6] Bullington, K., "Radio Propagation Fundamentals," Bell Syst. Tech. J., Vol. 36, 1957, pp. 593-626.
- [7] Bullington, K., "Phase and Amplitude Variations in

Multipath Fading of Microwave Signals," Bell Syst. Tech. J., Vol. 50, 1971, pp. 2039-2053.

- [8] Wozencraft, J. M. and I. M. Jacobs, Principles of Communication Engineering, John Wiley and Sons, New York, 1965.
- [9] H. B. Voelcker "Phase-Shift Keying in Fading Channels," Proc. Ins. Elec. Eng., Vol. 107, pt. B, Jan 1960, pp. 31-38.
- [10] G. D. Hingorani "Error Rates for a Class of Binary Receivers," IEEE Trans. Commun. Technol., Vol. COM-15, April 1967, pp. 209-215.
- [11] P. A. Bello and B. D. Nelin, "The Influence of Fading Spectrum on the Binary Error Probabilities of Incoherent and Differentially Coherent Matched Filter Receivers," IRE Trans. Commun. Syst., Vol. CS-10, June 1962, pp. 160-168.
- [12] J. J. Jones, "Multichannel FSK and DPSK Reception with Three - Component Multipath," IEEE Trans. Commun. Technol., Vol. COM-16, Dec. 1968, pp. 808-821.
- [13] J. C. Vanelli and N. M. Shehadeh, "Computation of Bit Error Probability Using the Trapezoidal Integration Rule," IEEE Trans. Comm., Vol. COM-22, pp. 331-334, March 1974.
- [14] E. J. Baghdady, Lectures on Communication System Theory, McGraw-Hill, New York, 1961.
- [15] M. Schwartz, W. R. Bennett and S. Stein, Communication Systems and Techniques, McGraw-Hill, New York, 1966.
- [16] Harry L. Van Trees, Detection Estimation and Modulation

- Theory," part 1, John Wiley and Sons, New York, 1968.
- [17] Papoulis, A., Probability, Random Variables and Stochastic Processes, McGraw-Hill, New York, 1965.
- [18] C. F. Lindman, Examen Des Nouvelles Tables D'intégrales Définies De M. Bierens De Haan, C. E. Stechert & Co., New York, 1944.
- [19] Gradshteyn, I. S. and I. M. Ryzhik, Table of Integrals, Series and Products, Academic Press, New York, 1965.
- [20] H. B. Dwight, Table of Integrals and Other Mathematical Data, McGraw-Hill, New York, 1965.
- [21] Eldon R. Hansen, A table of Series and Product, Prentice Hall Inc., 1975.
- [22] W. L. Miller and A. R. Gordon, "Numerical Evaluation of Infinite Series and Integrals Which Arise in Certain Problems of Linear Heat Flow, Electrochemical Diffusion, Etc.," Journal of Physical Chemistry, Vol. 35, Sep. 1931, pp. 2785-2884.
- [23] K. A. Karpov, Table of the Function $w(z) = e^{-z^2} \int_0^z e^{x^2} dx$
-
- in the Complex Domain, The Macmillan Company, New York, 1965.
- [24] Poisson, S. D., "Memoire sur le Calcul Numerique des Integrales Définies," Mem. Acad. Sc. Inst. France, Vol. 6, 1823, pp. 571-602.
- [25] Fettis, H. E., "Numerical Calculation of Certain Definite Integrals by Posson's Summation Formula," Math. Tables and Other Aids to Comp., Vol. 9, July

1955, pp. 85-92.

- [26] Erling D. Sunde, Communication Systems Engineering Theory, John Wiley & Sons, Inc., New York, 1969.
- [27] W. F. Walker, "The Error Performance of A Class of Binary Communications Systems in Fading and Noise," IEEE Trans. Commun. Technol., Vol. CS-12, March 1964, pp. 28-45.

APPENDIX A

DIGITAL COMPUTER PROGRAM TO CALCULATE TOTAL BIT-ERROR PROBABILITY FOR THE RAYLEIGH FAST-FADING CHANNEL

This program evaluates equation (64) for the total bit-error probability over a Rayleigh fast-fading channel using the trapezoidal integration method. The program is written in FORTRAN V for the Honeywell 66/60 digital computer. It will generate results for a range of sampling instants and signal-to-noise ratios as specified by the user. A listing of the main program and all subprograms is given in Appendix B1.

FORTRAN Variables and Constants

A tabulation of the variables and constants used in the programs is given in Appendix B2. The function of each quantity is stated, along with its FORTRAN name and the corresponding symbol used in the text of this report, where applicable.

Program inputs which must be supplied by the user are identified as such, and listed first in Appendix B2. These must be properly entered on cards according to the format specifications in the main program listing.

For each data point, the program prints out several of the variables in Appendix B2. These are identified as output data and are listed following the input data.

Program Operation

The first function of the main program is to read the input data. Then a subroutine, HSET, is called to compute the complete set of impulse responses, h_k , for a given sampling instant. The Gaussian and Chebyshev pulse shapes are programmed in function subroutine TIME, which is called by HSET.

At each sampling instant, P_e may be evaluated for several different signal-to-noise ratios. For each signal-to-noise ratio, the main program computes P_{e_0} , the probability due to additive noise alone, from (56).

Then, based on the specified error limit (10^{-14}), E_T , the integration step size and the signal-to-noise ratio, the number of points needed to evaluate (62) is determined. Function VFUN is called to compute the value of the integrand in (62) at each point; $n = 3$ is used for the series expansion in the expression of P_{e_z} . From these values the bit-error probability due to intersymbol interference, P_{e_z} , is determined. P_e is computed as the sum of P_{e_0} and P_{e_z} and the output is printed.

: Table B1. Listing of Digital Computer Program for the
Rayleigh Fast-Fading Channel

```

DOUBLE PRECISION V,TAU,TS,SIGN,H,HZERO,ERROR,ENOISE
DOUBLE PRECISION TAU1,DELTAU,SNRI,DELSNR,X,ERFCON,ERRISI
DOUBLE PRECISION DELTA,SNR,VFUNC,ERFC
DOUBLE PRECISION PI,TWOPI,SQRTWO,SQRTPI
COMMON/C1/TWOPI,SQRTPI,SQRTWO
COMMON/C3/H(100),HZERO
PI=.31415926535897324D1
TWOPI=PI*.2D1
SQRTPI=DSQRT(PI)
SQRTWO=DSQRT(.2D1)
DO 90 KKK=1,4
READ(5,405)TAU1,DELTAU,SNRI,DELSNR
READ(5,405)TS,DELTA,ERFCON
READ(5,404)MAXT,N1,N2,N3
TAU=TAU1-DELTAU
DO 1 K=1,N1
M=0
TAU=TAU+DELTAU
WRITE(6,994)
WRITE(6,997)TAU,TS,DELTA,ERFCON,MAXT,N1,N2,N3
CALL HSET(TAU,TS,MAXT,N3)
WRITE(6,999)
SNR=SNRI-DELSNR
DO 2 J=1,N2
SNR=SNR+DELSNR
SIGN=.1D2*(-SNR/.2D2)
X=ERFCON/DSQRT(.25D0*HZERO*HZERO+.5D0*SIGN*SIGN)
L=IDINT(X/DELTA)+2
ENOISE=.5D0-.5D0/DSQRT(.1D1+.2D1*SIGN*SIGN/HZERO/HZERO)
ERRISI=.0D0
V=.0D0
DO 3 I=2,L
V=V+DELTA
K1=I
ERRISI=ERRISI+VFUNC(V,SIGN,MAXT,K1,M)
3 CONTINUE
ERRISI=DELTA*.2D1*ERRISI
ERROR=ENOISE+ERRISI
WRITE(6,998)SNR,ENOISE,ERRISI,ERROR
IF(ERROR.LT..1D-9)GO TO 1
2 CONTINUE
1 CONTINUE
90 CONTINUE
404 FORMAT(4I5)
405 FORMAT(4D20.10)
997 FORMAT(1X,4D15.5,4I10////////)
994 FORMAT(1H1,100H          TAU          TS          DELTA
2   ERFCON          MAXT          N1          N2          N3/)
998 FORMAT(1X,4D15.5)
999 FORMAT(1X,60H          SNR          ENOISE          ERRISI
2   ERROR/)
STOP
END

```


Table B1. (continued)

```

SUBROUTINE HSET(TAU,TS,MAXI,N3)
DOUBLE PRECISION TAU,TS,TIME,T1,T2
DOUBLE PRECISION HZERO,H
COMMON/C3/H(100),HZERO
HZERO=TIME(TAU,TS,N3)
T1=TAU
T2=TAU
DO 1 K=1,MAXI
T1=T1-TS
T2=T2+TS
H(2*K-1)=TIME(T1,TS,N3)
H(2*K)=TIME(T2,TS,N3)
1 CONTINUE
RETURN
END

```

Table B1. (continued)

```

FUNCTION TIME(I,TS,N3)
DOUBLE PRECISION TIME,T,TS,X
TIME=.7D0
IF(N3.EQ.1)GO TO 3
IF(N3.EQ.2) GO TO 4
WRITE(6,220)N3
STOP
3 CONTINUE
X=.16D1*1/TS
IF(DABS(X).GT..5D1)GO TO 1
TIME=DEXP(-X*X)
1 CONTINUE
RETURN
4 CONTINUE
X=DABS(1)/13
IF(X.GT..2D2)GO TO 2
TIME=.4D23D0*DCOS(.2839D1*X-.7553D0)*DEXP(-.4587D0*X)
2 CONTINUE
IF(X.GT..4D2)RETURN
TIME=TIME+.7167D0*DCOS(.1176D1*X-.16D2D0)*DEXP(-.11D7D1*X)
220 FOR I=1,N3,27TIME DOES NOT EXIST FOR N3=,15)
RETURN
END

```

Table B1. (continued)

```

FUNCTION VFUNC(C,SIGN,MAXI,1,0)
  DOUBLE PRECISION HZERO,H,X,S,M1,X1,X2
  DOUBLE PRECISION PI,TWOPI,SORTWO,SORTPI,A
  DOUBLE PRECISION CHAR,V,SIGN,VFUNC,FACTL
  DIMENSION CHAR(2000),VSIN(2000)
  COMMON/C1/TWOPI,SORTWO,SORTPI
  COMMON/C3/H(100),HZERO
  IF(1.LE..000)GO TO 3
  S=1
  S=-.101
  NT=2*MAXI
  DO 1 K=1,NT
    J1=V+V+H(K)*H(K)
    IF(V1.LE..000)GO TO 1
    IF(V1.GT..501)GO TO 1
    S=-.000
    X1=-.101
    DO 2 N=1,2
      X1=-X1
    A=N-1
    S=S+X1*FACTL(A)/FACTL(.201*A+1)*V1**A
2 CONTINUE
    X=X*S
1 CONTINUE
    CHAR(I)=X
3 CONTINUE
    X2=-.2500*V+V*HZERO+HZERO-.500*SIGN*SIGN*V*V
    IF(X2.LE..-400)GO TO 4
    VFUNC=.500*(.101-CHAR(I))+DEXP(X2)*HZERO/SORTPI/.201
    RETURN
4 CONTINUE
    VFUNC=.000
    RETURN
END

```

Table B1. (continued)

```
FUNCTION FACTL(A)
  DOUBLE PRECISION FACTL, A
  FACTL = 1.0D1
  IF (A.LT..10D0) GO TO 10
  L = A
  DO 20 I = 1, L
20  FACTL = FACTL * I
  RETURN
10  RETURN
END
```

Appendix B.2. Program Variables and Constants for the
Rayleigh Fast-Fading Channel

FORTTRAN name	Function	Description or corresponding symbol used in text
DELSNR	Input	Signal-to-noise ratio increment in dB, per pass
DELTAU		Sampling instant increment per pass
DELTA		Δ
ERFCON		E_T will be on the order of $\text{erfc}(\text{ERFCON})$
MAXT		K
N1		Number of sampling instants desired
N2		Number of signal-to-noise ratios desired
N3		Use 1 for Gaussian pulse, 2 for the Chebyshev pulse
SNRI		Initial signal-to-noise ratio
TAUI		Initial sampling instant
TS		T
ENOISE	Output	P_{e0}
ERRISI		P_{ez}
ERROR		P_e
SNR		ρ
TAU		γ
FACTL	Internal	Function subprogram name
HSET		Subroutine name
TIME		Function subprogram name
VFUNC		Function subprogram name

Appendix B2. (concluded)

FORTTRAN	Function	Description or corresponding symbol used in text
CHAR	Internal	$M_Z(\lambda)$
H		h_k
HZERO		h_0
I,J,K,K1,M		Dummy integer variables
PI		π
SIGN		σ_n
SQRTPI		$\sqrt{\pi}$
SQRTWO		$\sqrt{2}$
T		t
TWOPI		2π
T1,T2		$\gamma - kT, \gamma + kT$
V		λ
X,X1,X2,Y,Z	✓	Dummy real variables